Review Article

Menghao Chen#, Chengfeng Luo#, Ying Yuan, Hao Zhou, Zhanglong Li, Qiang Wang, Baijuan Gong*, Zhimin Li*, and Hongchen Sun

Modification of PEEK for implants: Strategies to improve mechanical, antibacterial, and osteogenic properties

https://doi.org/10.1515/rams-2024-0025
received November 30, 2023; accepted April 22, 2024

Abstract: Poly-ether-ether-ketone (PEEK), a biomaterial renowned for its mechanical prowess and biocompatibility, is increasingly preferred for medical implants. Its natural bone-like mechanical property, ease of manipulation, and ability to mitigate stress shielding render it a standout replacement for titanium in dental implantology. Adding carbon fiber and graphene to PEEK can further enhance the mechanical properties of PEEK. However, the biological passivity of PEEK hampers its efficacy in bone repair, driving spurring research into surface modifications to enhance its bioactivity. Incorporating metal, inorganic, and organic antimicrobial agents is anticipated to bolster PEEK's resistance to bacteria, thereby reducing the risk of acute postoperative infections and peri-implantitis. Apart from its antimicrobial activity, researchers have also investigated methods to enhance the osteogenic properties of PEEK. These approaches include surface modification and blending modification. Surface modification includes physical modification, chemical modification, and biologically active substance modification. These methods can further enhance the implant integration and durability, potentially improving patient outcomes. This overview examines PEEK's processing techniques and highlights recent research achievements in improving its biomechanical, antibacterial, and osteogenic properties. Considering these strides, we argue that modified PEEK holds significant promise as a material for dental implants, charting an encouraging course for its clinical future.

Keywords: PEEK, 3D printing, antibacterial, osseointegration, modification

1 Introduction

Periodontitis, dental caries, tumors, and accidents have contributed to an increasing clinical demand for dental restoration and bone defect materials in modern stomatology [1]. Currently, metallic, ceramic, and polymer materials are the primary materials used in tooth restoration and maxillofacial restoration in clinical practice. Ceramic materials are preferred for their pleasing aesthetics, durability, and comfort [2]. However, ceramic materials exhibit lower strength and greater brittleness [3]. Metallic biomaterials, including titanium (Ti) and Ti alloys, are widely used as permanent implants due to their high mechanical strength [4]. But metal implants have a higher elastic modulus and can release metal ions, which may lead to bone resorption, gingival discoloration, and allergic reactions in some patients [5]. These factors have spurred the need for the development and improvement of new materials in the fields of dentistry and orthopedics [6]. In recent years, poly-ether-ether-ketone (PEEK) has attracted extensive attention from researchers.

PEEK, part of the polyaryletherketone family, is a two-phase semi-crystalline polymer composed of repeating units featuring a single ketone bond and double ether

# These authors contributed equally to this work and should be considered first co-authors.

*** Corresponding author: Baijuan Gong,** School of Stomatology, China Medical University, Shenyang 110002, China; Liaoning Provincial Key Laboratory of Oral Diseases, Shenyang 110002, China, e-mail: bjgong@cmu.edu.cn
*** Corresponding author: Zhimin Li,** School of Stomatology, China Medical University, Shenyang 110002, China; Liaoning Provincial Key Laboratory of Oral Diseases, Shenyang 110002, China, e-mail: zmli@cmu.edu.cn
Menghao Chen, Chengfeng Luo, Ying Yuan, Hao Zhou, Zhanglong Li, Qiang Wang: School of Stomatology, China Medical University, Shenyang 110002, China; Liaoning Provincial Key Laboratory of Oral Diseases, Shenyang 110002, China
Hongchen Sun: School of Stomatology, Jilin University, Changchun, 130021, China

bonds in its main chain [7]. PEEK is a notable high-performance engineering plastic that is widely known for its multitude of exceptional properties [8]. These attributes include high heat resistance [9], excellent machinability, favorable biocompatibility, and excellent X-ray penetration capability [10]. PEEK's molecular structure features a benzene ring, which provides rigidity, and ether bonds that contribute to its ample toughness, making PEEK exceptionally resistant to cyclic stress [11]. PEEK is capable of overcoming some limitations associated with metal implants, such as metal allergies [12]. Notably, PEEK's elastic modulus (3 GPa) closely resembles that of human bone (3–17 GPa), enabling it to effectively mitigate the "stress shielding" issue at surgical sites and reduce the risk of osteoporosis (Table 1) [13]. Due to these exceptional properties, PEEK has emerged as a substitute for metal implants and a replacement material for orthopedic and trauma surgery since the late 1990s [14]. In present clinical practice, PEEK is extensively utilized as a dental and orthopedic material (Figure 1), and it has demonstrated favorable outcomes [15]. PEEK materials have been increasingly used clinically in various dental applications, including fixed clasps, fixed bridges, dental crowns, implant abutments, and implant restoration materials [16].

However, the molecular structure of PEEK makes it highly hydrophobic, leading to reduced cell adhesion functionality, thus classifying PEEK as a biologically inert material [29]. While PEEK has been widely used in hard tissue implants, its biological inertness can lead to slower bone healing and even implant loosening [30]. On the other hand, bacterial infection at the implant site is another common clinical complication [31]. If not properly managed, infection can cause pain, delayed wound healing, and even implant failure, posing a significant risk to patients [32]. With increasing numbers of bone grafting surgeries, strategies to address these issues have become crucial. As a result, many recent studies in this field have shifted the focus from improving the biomechanical properties of PEEK to promoting osseointegration and implant infection control, which are vital for the long-term success of implants. Therefore, this review aims to summarize PEEK's processing methods and the recent progress of PEEK modification technology, especially in terms of antibacterial properties and osseointegration functions.

2 PEEK manufacturing technology

Having a glass transition temperature (T_g) of 143°C and a melting point (T_m) of 343°C, PEEK exhibits a markedly superior melting temperature when compared to standard thermoplastics [33]. This melting point emphasizes the necessity for processing techniques capable of withstanding elevated temperatures [34]. Currently, the processing of PEEK involves both conventional and additive manufacturing techniques [35]. The traditional methods include injection molding, hot pressing molding, extrusion molding, and centrifugal molding. Injection molding entails heating the material to a high temperature until it becomes molten, which is then injected into a designed mold and cooled to form a product of a specific shape [37]. This stands as a frequently utilized approach for processing PEEK. This technique typically necessitates minimal post-processing, often involving the removal of rough edges and trimming of excess plastic [38]. Injection molding is well-suited for the fabrication of thin-walled components and for producing intricate parts with precise and delicate details. Furthermore, components manufactured through this process feature a commendable surface finish and exhibit exceptional

Table 1: Elastic modulus of bone and bone substitute materials

Materials	Types	Tensile strength (MPa)	Flexural strength (MPa)	Young's modulus (GPa)	Ref.
Cancellous bone	Human bone	13–17	12–18	2–4	[17]
Cortical bone	Human bone	105–115	118–122	27–33	[18]
PEEK	Nondegradable polymer	86–94	110–120	3–4	[19]
20 wt% CFR–PEEK	Nondegradable polymer	125–131	160–168	18–20	[20]
30 wt% CFR–PEEK	Nondegradable polymer	151–157	163–173	22–28	[21]
GFR–PEEK	Nondegradable polymer	115–158	198–228	10–12	[22]
Magnesium	Degradable metal	190–210	69–105	40–45	[23]
Solid tantalum	Nondegradable metal	290–320	230–350	100–186	[24]
Ti	Nondegradable metal	460–470	317–323	110–120	[25]
316L SS	Nondegradable metal	272–356	220–250	190–230	[26]
Co–Cr alloys	Nondegradable metal	751–815	565–597	170–210	[27]
ZrO_2	Nondegradable metal	320–340	240–260	200–210	[28]

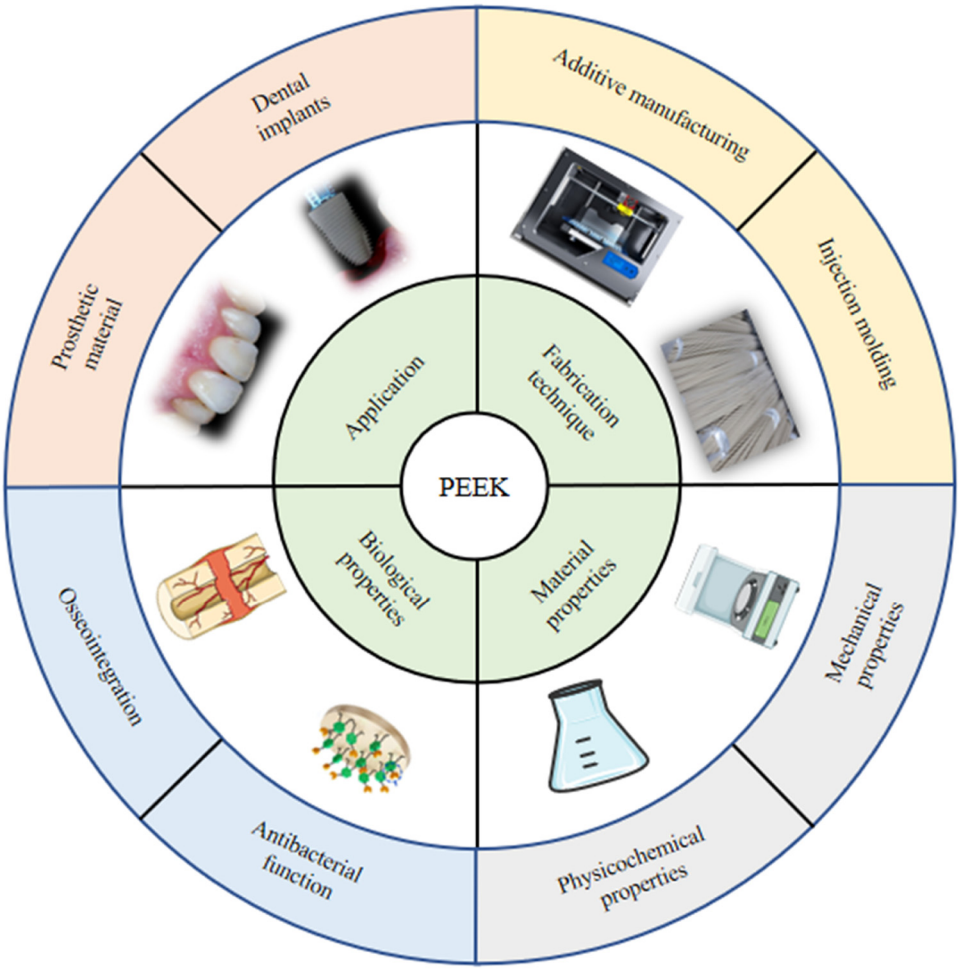

Figure 1: Basic and applied research of PEEK in medical material.

dimensional accuracy [39]. From a production perspective, notable advantages include heightened productivity and reduced labor expenditures. However, the flip side entails the drawback of elevated overall costs. Hot pressing refers to the direct processing of the material in the mold through pressure and temperature. Once the component has cooled, it is extracted from the mold and subjected to a flashing procedure. This process is the standard manufacturing method for making parts from PEEK [40]. Components fabricated using this method exhibit a favorable surface finish. This method features a very fast setup time and relatively low setup cost. Nevertheless, it is not capable of handling geometries featuring undercuts, and both processing time and part consistency need to align with the standards achieved through injection molding. Extrusion is applied in the production of polymer components characterized by a consistent cross-section, such as PEEK tubes. This represents another prevalent manufacturing method for crafting PEEK components. The heated plastic material is shaped under elevated pressure within an open mold. This method is cost-effective to produce, with quick setup times and relatively low initial costs. However, the precision is lower than that of injection molding, and it is only suitable for parts with a uniform cross-section. Centrifugal molding is another technique employed in the processing of PEEK [41]. This technique involves placing PEEK material into the mold and subsequently sealing it. The mold is heated, causing the PEEK to melt. Subsequently, the mold is rotated along multiple axes. Centrifugal force ensures uniform polymer distribution along the mold's inner surface. This method is used to manufacture complex hollow parts with thin walls and extremely low residual stresses. Centrifugal molding provides a superb surface finish while incurring minimal tooling expenses. It is well-suited for both short and long production runs (Figure 2). Its primary drawbacks include reduced precision and slower production speeds in comparison to injection molding (Table 2).

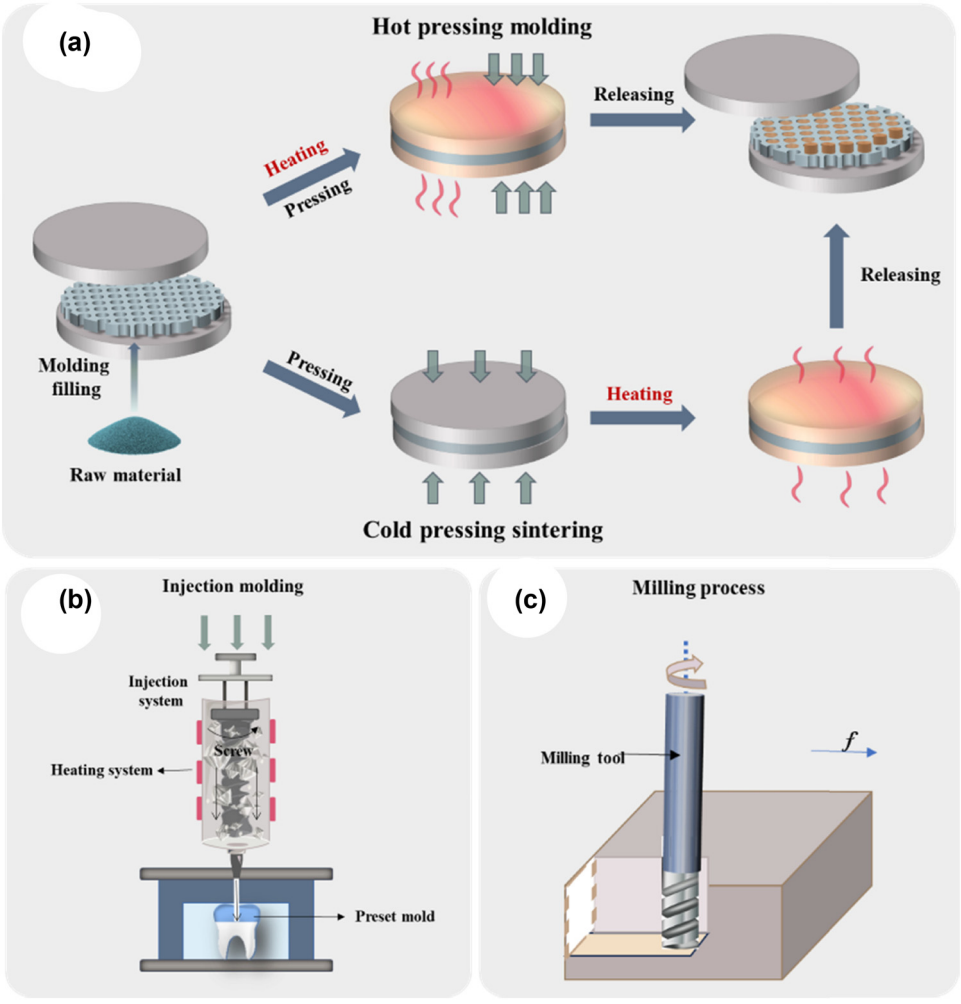

Figure 2: PEEK's traditional processing methods. (a) Schematic diagram of compression molding: hot pressing molding and cold pressing sintering. (b) Schematic diagram of injection molding. (c) Schematic diagram of cutting and molding.

Table 2: Manufacture methods of PEEK

Process methods	Advantages	Disadvantages	Ref.
Injection molding	Fast production speed Suitable for mass production	Limited shape and size High operating requirements	[42]
Hot pressing	Low cost of equipment	Poor accuracy Difficult to control thickness	[43]
Extrusion molding	Low cost Fast productivity	Poor accuracy Narrow scope of application	[44]
Centrifugal molding	High surface polish Low cost	Poor accuracy Low productivity	[45]
SLS	High precision Complex structure of the product can be constructed	High cost High requirements for printing environment	[46]
FDM	Low cost	The interlayer binding force of the product is weak	[47]
SLA	High accuracy	Only available for photopolymers	[48]

Furthermore, additive manufacturing techniques have also been employed for processing PEEK in recent years [49]. Additive manufacturing, commonly referred to as 3D printing technology, emerged as an innovative manufacturing method in the late 1980s [50]. It operates by sequentially depositing materials layer by layer to fabricate three-dimensional structures. Initially, the user utilizes computer-aided design software for modeling [51]. Subsequently, the user imports the data (in STL format) generated by the design software into the 3D printer, which then fabricates the object layer by layer. The additive manufacturing methods suitable for processing PEEK primarily include selective laser sintering (SLS) and fused deposition modeling (FDM), each with its own set of advantages and disadvantages. SLS is a 3D printing method that utilizes laser energy for powder sintering [51]. Its principle involves spreading powder on a platform and utilizing laser energy to fuse the material, thereby constructing a shape according to a pre-programmed design. The advantages of using this technology for producing PEEK medical products include rapid printing speed, exceptional printing accuracy, and a resolution reaching 50–100 μm. The drawback includes intricate equipment manufacturing process, elevated printing expenses, and the demanding printing environment. FDM can also print oral medical devices made of PEEK. It functions by extruding PEEK filaments from the nozzles of the 3D printing device, building the model layer by layer. The advantages of FDM are low printing cost, simple equipment manufacturing, the ability to print at room temperature, and strong model controllability [52]. However, there are currently reports that this technique produces PEEK products with weaker internal bond strength due to higher nozzle temperatures. This occurs because excessively high temperatures can affect the crystallization process of the product, and subsequently affect the mechanical properties of the product [53]. Thankfully, a controlled cold deposition technique has recently been developed to address this problem, thereby enhancing the possibilities of FDM for medical PEEK material applications (Figure 3).

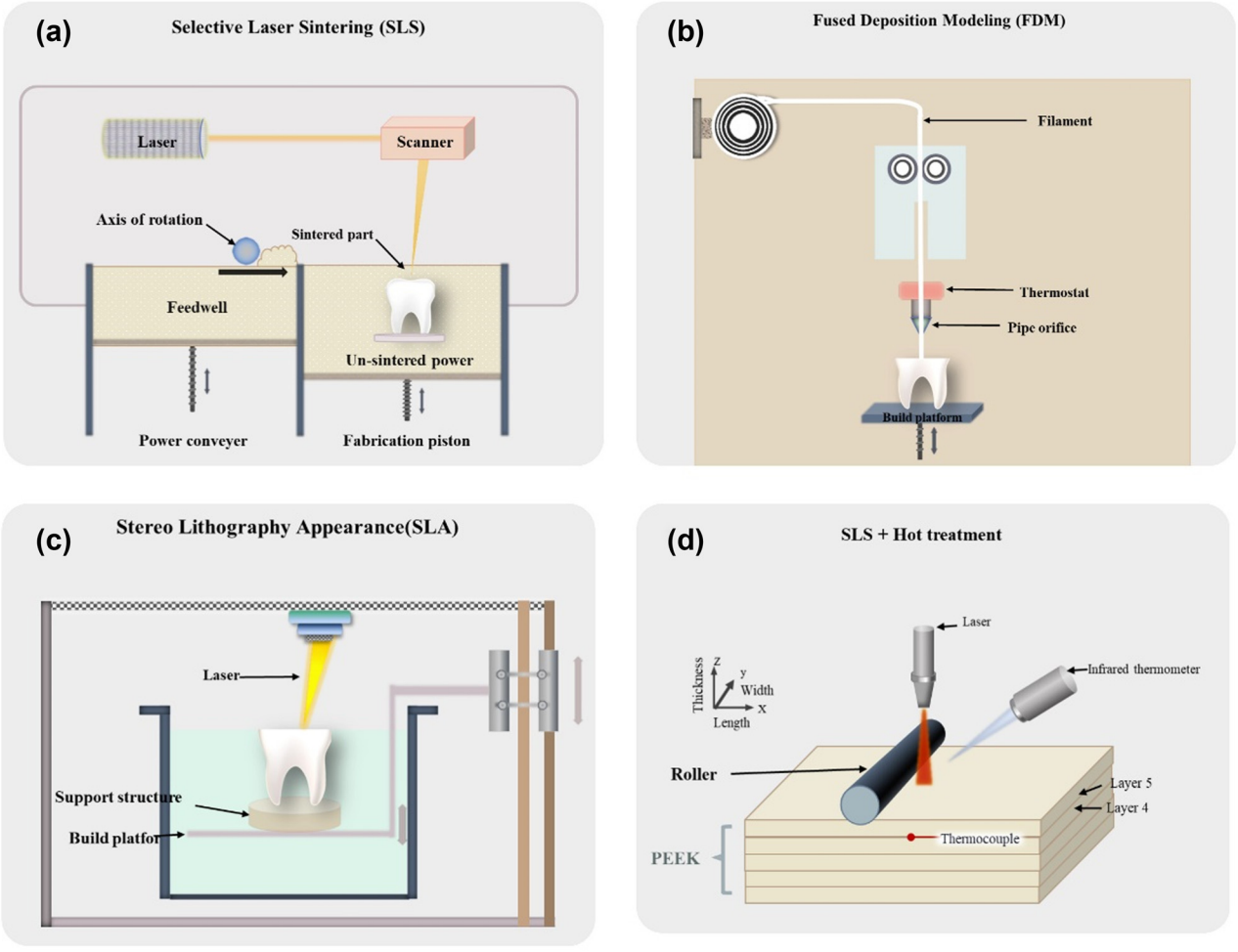

Figure 3: PEEK's additive manufacturing methods: (a) SLS, (b) FDM, (c) stereo lithography appearance (SLA), and (d) SLS + hot treatment.

3 Enhancing the mechanical properties of PEEK

PEEK, a high performance engineering plastic, was pioneered by British Imperial Chemical Industries in 1978 [54]. It is a semi-crystalline aromatic polymer that is renowned for its distinctive attributes, which include physical and chemical properties, as well as mechanical characteristics [55]. These inherent traits form the foundation for the utilization of PEEK materials in dental and orthopedic implants (Figure 4).

PEEK is a remarkable material with outstanding physical and chemical properties, making it particularly well-suited for implantable medical devices and applications [56]. Its unique combination of characteristics enhances the safety and effectiveness of such devices. PEEK's exceptional temperature resistance is a standout feature. With a high glass transition temperature (T_g) of approximately 143°C and a melting point (T_m) of around 343°C, PEEK can withstand the physiological temperature in the human body without losing its structural integrity [57]. This quality ensures the longevity and reliability of implants even in challenging physiological environments. PEEK's low density, approximately 1.32 $g \cdot cm^{-3}$, is advantageous for implantable devices, as it reduces the overall weight of the device, thus minimizing the burden on the patient [58]. Additionally, PEEK's minimal solubility and water absorption further contribute to its biocompatibility, preventing adverse reactions within the body [59]. From a chemical perspective, PEEK's resistance to corrosion and hydrolysis is essential for implantable medical devices that must maintain their structural integrity over extended periods. Its stability in the presence of bodily fluids and chemicals ensures the longevity of implants, reducing the need for frequent replacements and associated surgical procedures. In environments with pH levels of 3, 7, and 10, the fatigue mechanical properties of PEEK remain consistent [60]. Furthermore, PEEK's ability to resist radiation,

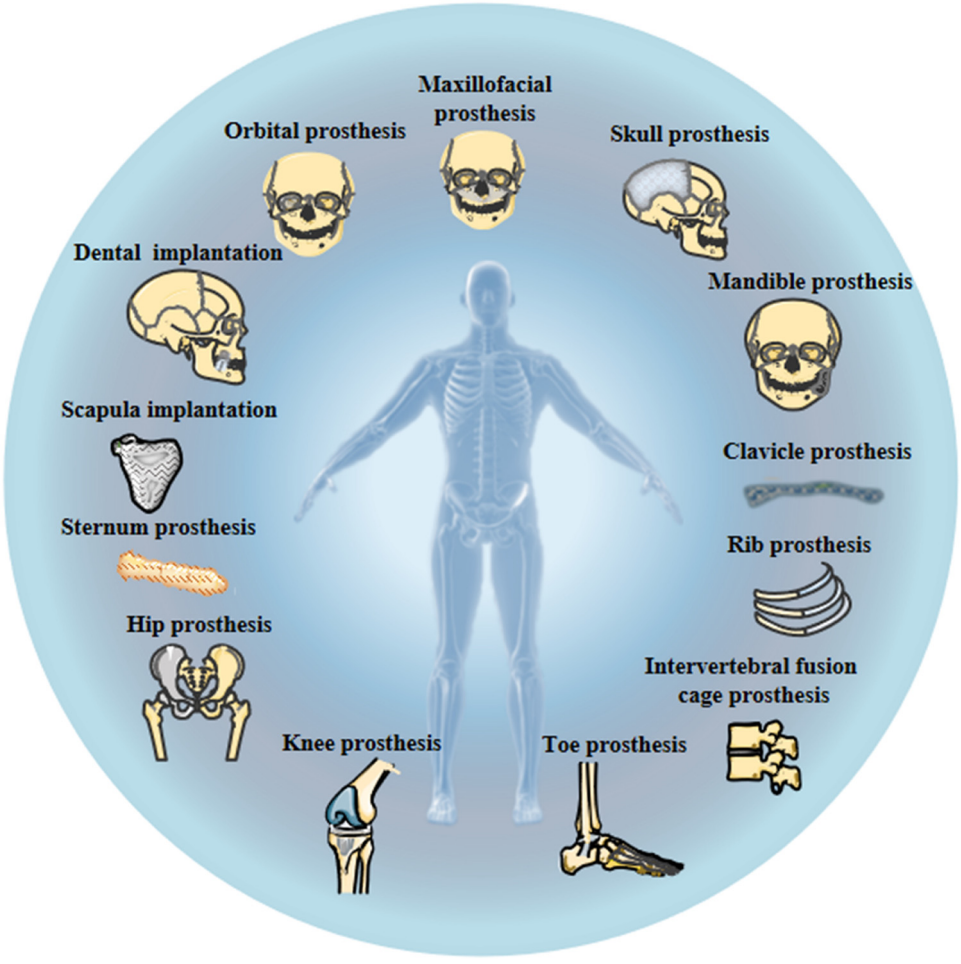

Figure 4: Application of PEEK in orthopedics and stomatology.

including electron beam and gamma radiation, makes it suitable for applications requiring sterilization and long-term functionality [61].

In terms of mechanical properties, PEEK offers an impressive balance of stiffness and flexibility, closely resembling the mechanical properties of natural bone [62]. This makes it an excellent choice for orthopedic implants, as it minimizes the risk of stress shielding and provides long-term stability. Ensuring that the mechanical properties of an implant closely match those of human bone is crucial for its long-term success in orthopedic and dental applications. PEEK, with a modulus of 3–4 GPa like that of the more flexible cancellous bone, falls slightly short of matching the modulus of cortical bone, which ranges from 25 to 30 GPa. To address this challenge, an effective strategy involves enhancing the mechanical characteristics of PEEK through various modifications, including the incorporation of additional phases such as carbon fibers (CFs), carbon nanotubes (CNTs), and graphene oxide (GO) [63]. The primary objective is to achieve a uniform dispersion of these fillers within the polymer matrix and enhance the interface bonding between the inorganic and organic components.

The addition of CFs to PEEK brings about a significant improvement in mechanical performance. CFs, well-known for their high strength and modulus, act as excellent reinforcement materials for PEEK. When the CF content is relatively low, typically below 10 vol%, CFs disperse uniformly within the PEEK matrix, resulting in a linear increase in tensile stiffness and strength while preserving PEEK's ductility [64]. When the CF content exceeds a certain threshold, the composite material is often more vulnerable to acid corrosion, exhibits stronger brittle behavior, and displays pronounced piezoresistive behavior. In addition, the material experiences higher levels of inelastic deformation and reduced resistance to impact damage when compared to pure PEEK [65,66]. However, this brittleness can be mitigated by precisely controlling the ratio, size, orientation, and interface of CFs, such as continuous long CFs introducing anisotropic mechanical properties into the composite, which means that its mechanical properties vary with the loading direction. Conversely, randomly oriented short CFs create isotropic behavior in the composite. Short CFs offer the advantage of better dispersion within the PEEK matrix, ensuring uniform properties throughout the material [67]. Such adaptability allows CF/PEEK composites to closely match the biomechanical properties of host bone tissue, making them ideal for orthopedic applications. Nevertheless, due to the chemical inertness and hydrophobicity of CF and PEEK and their insufficient active groups, the composite delaminates, reducing significantly the interlaminar shear strength and fatigue resistance of the composite and limiting its application [68]. Therefore, enhancing the interfacial bonding strength is crucial to optimize the mechanical properties of CF/PEEK composites. Strategies aimed at improving interfacial interactions include enhancing intermolecular forces, establishing chemical bonds, and promoting mechanical interlocking. Techniques like introducing PEEK as interface layers on activated CFs and employing polyetherimide (PEI) and GO complex sizing on CF surfaces [69], and the direct spraying of treated CNTss to CF/PEEK prepreg by prepreg spraying method have all shown promising results in enhancing interfacial bonding and, consequently, mechanical properties [66,70,71]. Shifting focus to CNTs, these materials possess exceptional mechanical and physical properties, making them ideal for use as fillers in composites. Upon adding CNTs to PEEK, parameters such as Young's modulus, tensile strength, flexural modulus, and flexural strength are improved, effectively enhancing the mechanical properties of PEEK [72,73]. With the addition of CNTs, the material's stiffness is significantly enhanced, while its ductility is reduced. Additionally, the wear resistance is significantly improved, with the optimal wear resistance of the composite observed at the low content of CNTs (5 vol%) [74]. In various types of CNT fillers, especially single-walled CNTs (SWCNT) is a very effective additive, in PEEK to add a small amount of SWCNTs, in addition to improving mechanical properties, due to the Van der Waals force between carbon atoms, the antioxidant effect of CNTs can also improve their heat resistance, and the use of large-diameter, small-diameter SWCNTs, as well as high-mass fraction SWCNTs, can also improve the effective thermal conductivity of composite materials [75]. However, the tendency of CNTs to aggregate into bundles due to Van der Waals forces can hinder their dispersion within a polymer matrix. Multi-walled CNTs (MWCNTs), with weaker Van der Waals forces, exhibit reduced aggregation tendencies. Research indicates that the introduction of MWCNTs significantly enhances the Young's modulus of PEEK composites, but the binding force between MWNTs and PEEK matrix is weak [73]. Therefore, various methods have been employed to improve CNT dispersion, including *in situ* polymerization, covalent grafting, deposition of nanocomposite coatings on PEEK surfaces [76], and establishing hydrogen bond interactions between functionalized PEEK and CNTs. It is worth noting that CNTs have needle-like properties that can damage human organs [70]. GO, a graphene derivative rich in oxygen functional groups, has emerged as another valuable addition to PEEK. Mechanical testing has indicated that the reinforced composite's toughness changes with the GO content. At 0.5% GO, it achieves maximum elongation at break while still sustaining its compression modulus. The improved mechanical properties of the

material are due to the uniform dispersion of GO in the matrix and the strong π–π interaction between the large π-conjugate structure of GO and the benzene ring in PEEK [77]. However, excessive GO content may cause uneven dispersion and ultimately reduce toughness, negatively impacting the mechanical properties [78]. At present, the understanding of the nature of GO is still not comprehensive, and its lack of stability greatly hinders its application in orthopedics [79]. For this reason, the mechanical characteristics, bactericidal properties, and osteogenesis-promoting ability of GO are now optimized by using polymeric and non-polymeric precursors for multiplex plasma treatment [79], multifunctional nano-coatings consisting of GO nanosheets, polydopamine (PDA) nanolayers and basic fetoprotein (BFP) oligopeptides on orthopedic PEEK implants [80], and GO-modified microporous/nano-porous PEEK biomaterials [81]. In summary, the introduction of CFs, CNTs, and GO into PEEK composites induces significant alterations in their mechanical properties, making them highly suitable for orthopedic applications. These modifications enable PEEK-based composites to strike a delicate balance between robust mechanical strength and biocompatibility, positioning them as promising candidates for a wide range of orthopedic implant applications. Further research and refinement of these composite materials hold great potential for revolutionizing dentistry and orthopedics.

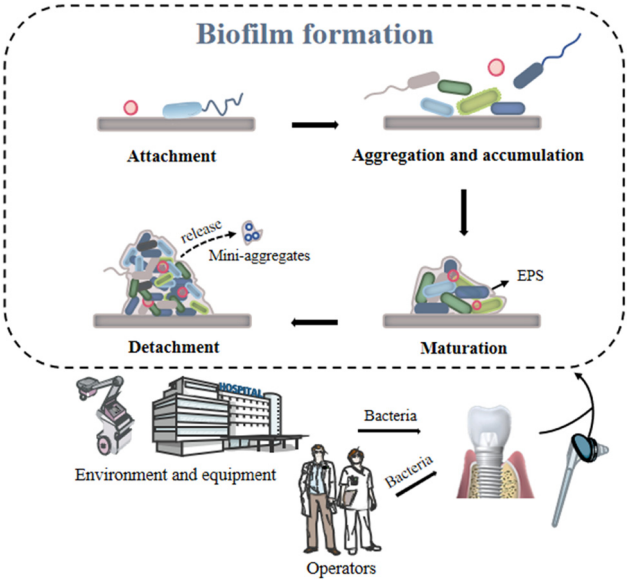

Figure 5: Schematic diagram of the biofilm formation process after bacterial adhesion to the surface of the implant and the source of implant-related infection. Bacteria from the operators, operating environment, and operating equipment adhere to the surface of the implant, aggregate and accumulate, and form EPS. The bacteria covered by EPS gradually mature and continue to secrete EPS, and the biofilm matures to attract more bacterial adhesion. The aggregates of bacteria begin to decompose into mini-aggregates and then are released. EPS: extracellular polymeric substances.

4 Strategies for increasing the antibacterial activity of PEEK

Currently, thousands of implants are employed in stomatology annually, and a portion of these implants could undergo bacterial colonization [82]. Postoperative acute infections and peri-implantitis are prevalent complications associated with oral medical implants. These issues also constitute significant factors contributing to long-term discomfort, loosening, or even implant failure subsequent to implant surgery [83]. Indeed, a crucial element in oral implant infections is the adherence of bacteria to the implant surface and the subsequent creation of a biofilm within the oral environment. This distinctive biofilm structure can result in varying degrees of damage to the surrounding tissues of the implant (Figure 4) [84]. The oral cavity constitutes a significant ecological niche for the colonization and persistence of human microorganisms [85]. Among these, the oral microbiota ranks as the second-largest microbial community following the intestinal microbiota, encompassing over 700 distinct microorganisms [86]. While adhering to rigorous aseptic procedures, the introduction of pathogenic bacteria during implantation is unavoidable [87]. Bacterial colonization, proliferation, and maturation progressively give rise to the development of bacterial biofilms [88]. Various varieties of bacteria, proteins, and sugars are found within plaque biofilms [89]. These components, such as cell wall teichoic acid of gram-positive bacteria and lipopolysaccharide released by gram-negative bacteria, as well as various proteolytic enzymes, can cause implant infection (Figure 5) [90]. To tackle these potential concerns, the development of implant materials endowed with antimicrobial attributes holds significant importance. To date, antibacterial-modified PEEK is a promising dental implant material.

4.1 Antibacterial metal particles

Many metal elements with antibacterial properties, such as Ag, Cu, Zn, Mn, and Fe, have been enriched on the surface of PEEK, which allows the implant to have antibacterial capabilities. They can inhibit or even kill the bacteria by destroying bacterial cell membranes, destroying proteins and DNA within the bacteria, and producing reactive

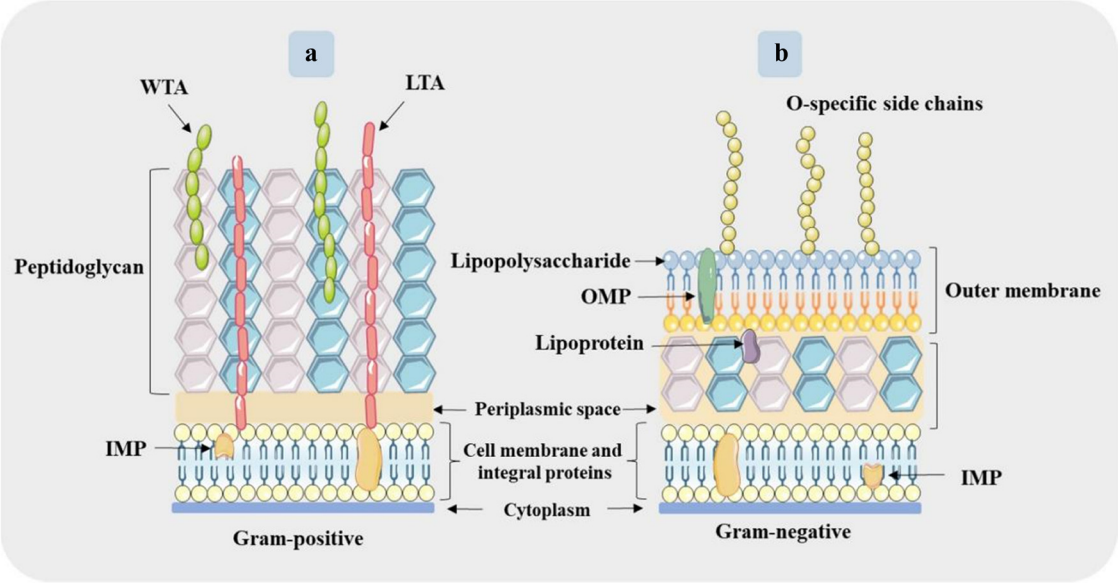

Figure 6: Schematic diagram of the cell wall: (a) gram-positive bacteria and (b) gram-negative bacteria. WTA: wall teichoic acid; IMP: integral membrane protein; LTA: lipoteichoic acid; OMP: outer membrane protein.

oxygen species (ROS) (Figure 6) [91]. Antibacterial metal ions, such as silver ions, have been applied to PEEK to deal with potential infection problems in oral implants. Silver, a common disinfectant for thousands of years of human history, has toxic effects on a variety of microorganisms while its toxicity to humans is minimal and insignificant [92]. It has been demonstrated to disrupt bacterial metabolism through various mechanisms [93]. Silver ions can penetrate bacterial cell walls and cell membranes, and then enter the combination of cells and ribosomes to inhibit protein synthesis [94]. In addition, silver can also destroy the oxidative respiratory electron transmission chain by losing respiratory enzymes on the cell membrane [95]. More importantly, silver ions produce ROS to lead bacterial cracking death eventually. The silver ions of appropriate concentration have good antibacterial capabilities due to these mechanisms. Liu *et al.* employed the magnetic sputtering method to create a nano-silver coating on the PEEK. The experimental findings indicated that PEEK with a silver-coated surface exhibited no cytotoxicity, and the water contact angle experienced a notable increase. Moreover, the antimicrobial efficacy of PEEK with a silver coating exhibited significant enhancement compared to pure PEEK [96]. Deng *et al.* utilized dopamine chemistry to create silver-modified 3D printed PEEK. Cell experiments demonstrated that the modified material had the capacity to enhance the proliferation and differentiation of MG-63 cells. Additionally, the modified material exhibited a substantial antibacterial impact on both *Escherichia coli* and *Staphylococcus aureus* [97]. Jerome Girard *et al.* synthesized a PEEK with pyridine side groups to integrate silver ions into the polymer. This modified material also has a good inhibitory effect on *S. aureus*, *E. coli*, and other gram-negative and gram-positive bacteria. It is an ideal new PEEK material with antibacterial function [98]. Furthermore, Yu *et al.* employed PDA to uniformly incorporate silver ions onto the PEEK surface. Subsequently, they applied a spin-coated carboxymethyl chitosan film (CMC) that regulated the release of silver ions and synergistically exhibited antibacterial properties. *In vitro* antibacterial experiments demonstrated that the modified PEEK exhibited effective antibacterial effects against both gram-negative and gram-positive bacteria [99]. In addition, silver ions can also be used in combination with nano-SiO_2. SiO_2 has a porous structure, which allows the slow release of silver ions. A two-layer coating was prepared on stainless steel (SS) by Nawaz *et al.* The first layer adopts electrophoretic deposition to prepare bioactive glass nanoparticles (MBGN)/bioactive glass BG/PEEK composite coating. The second layer was deposited on Ag/nSiO_2 using radio frequency co-sputter deposition (RF). RF deposition for 20 min and 40 min gave SS–PEEK/BG/MBGN–Ag/nSiO_2 (RF20) and SS–PEEK/BG/MBGN–Ag/nSiO_2 (RF40). Both materials have certain antimicrobial properties [100]. Nawaz *et al.* synthesized 5–6 μm thick porous bioactive glass coatings with silver–manganese elements (Ag–Mn–MBGNs) on PEEK/bioactive glass coatings (PEEK/BG). This material, PEEK/BG–Ag/Mn/MBGNs, has antibacterial effects against gram-positive and gram-negative bacilli. This is also related to silver ions [101]. Although silver ions have outstanding antibacterial functions, some studies have shown that excessive

silver ions have toxic side effects on mammalian cells [102]. It can disrupt the respiratory electron transport chain of mitochondria in normal cells, leading to the production of ROS, leading to DNA fragmentation [103]. Therefore, implants containing silver ions need to add an appropriate amount of silver, while obtaining good antibacterial activity, it will not have adverse effects on the metabolism of normal cells.

Other metal ions, such as Cu ions, are also significant antibacterial agents. Copper serves as a vital co-factor for numerous essential enzymes engaged in the electron transport chain of cellular oxidative respiration, including cytochrome c oxidase and ceruloplasmin [104]. Yan *et al.* employed dopamine chemistry to coat silver nanoparticles onto the surface of copper oxide microspheres (CuO), subsequently applying the composite microparticles (CuO/Ag) onto porous PEEK surfaces with the aid of silk fibroin. *In vitro* antibacterial tests revealed that the modified PEEK displayed a beneficial antibacterial impact and effectively restrained biofilm formation [105]. Under the local acidic environment (pH = 5.0) simulating bacterial survival, the killing rate of modified PEEK to *E. coli* reached 99.99%. This modified PEEK possesses robust antibacterial capabilities attributed to distinct antibacterial mechanisms involving silver ions and copper ions. Regarding the cell membrane, silver ions can disrupt it by attaching to specific sites on the membrane, disrupting the bacterial membrane's oxidative electron transport chain [106]. On the other hand, copper directly engages in a lipid peroxidation reaction with the cell membrane. Concerning intracellular active oxygen, silver ions indirectly contribute to heightened active oxygen levels by consuming antioxidant substances [107]. Meanwhile, copper catalyzes Fenton reactions and hydroxyl free radical reactions, directly resulting in active oxygen generation. Concerning bacterial proteins, silver has the capability to displace regular metal ions in bacterial proteins, resulting in protein loss [108]. Conversely, copper induces protein denaturation by oxidizing amino acid side chains within the protein. Currently, researchers posit that copper ions can engage in disrupting cell membranes, altering intracellular biochemical processes, and inducing DNA damage [109]. These cumulative effects ultimately result in bacterial cell death [110]. For instance, Liu *et al.* used magnetron sputtering to sputter Cu nanoparticles on PEEK. *In vitro* experiments reveal that the copper-coated modified PEEK demonstrates a potent bactericidal effect *via* the mechanisms of "contact inhibition" and "induced killing." This effect is attributed to the copper ion-induced polarization of macrophages. The presence of copper ions induced the conversion of macrophages from the M0 phenotype to the M1 phenotype, resulting in enhanced macrophage phagocytosis of methicillin-resistant *S. aureus* [111]. Yan *et al.* deposited copper citrate nanoclusters on porous PEEK using PDA technology. *In vitro* experiments showed that 93% of planktonic bacteria were destroyed. This shows that the material has the potential to kill bacteria and control infection. This is because the presence of citrate promotes the transport of copper ions into the cells, increases the copper content in bacterial cells, and then generates active oxygen to destroy bacteria. PDA coatings can release high doses of copper at low pH in the presence of bacteria [112]. Wang *et al.* coated Mn^{2+} and Cu^{2+} on the PEEK surface with PDA. This modified PEEK can inhibit *S. aureus* and *E. coli*. This antibacterial effect is related to copper ions [113].

Iron also has some antibacterial properties. Iron is a vital trace element essential for bacterial survival, playing key roles in processes such as bacterial DNA synthesis and energy metabolism. However, an excess of iron can prove detrimental, potentially leading to the demise of bacteria [114]. In physiological settings, iron predominantly exists in two states: the oxidized form Fe^{3+} (ferric iron) and the reduced form Fe^{2+} (ferrous iron) [115]. Bacteria will reduce external Fe^{3+} to more soluble Fe^{2+}. Fe^{2+} produces a large amount of OH^- through the Fenton and Haber-Weiss reaction [116]. These free radicals cause bacterial damage by peroxidizing lipids in cell membranes and introducing harmful proteins and damaging DNA. Zhang *et al.* constructed a composite coating ($CuFe_2O_4$/GO) of two-dimensional GO and photo-activated copper ferrite (PEEK–$CuFe_2O_4$/GO), and this antibacterial coating with photosensitive properties was applied on PEEK [117]. Under the action of near-infrared light at 808 nm, the material produced strong antibacterial properties. This is related to the copper ions and iron ions released by $CuFe_2O_4$. Iron and copper ions undergo glutathione depletion and Fenton reaction in infected environments. This produces OH^- and causes damage to the internal structure of the bacteria [118].

Besides these elements, nano-zinc also plays an important role as antibacteria. A possible antibacterial mechanism of zinc ions is to induce cells to produce ROS, which leads to bacterial cell wall damage and enhanced membrane permeability, thereby inhibiting bacterial growth [119]. Zinc serves as a comprehensive antibacterial agent without inducing bacterial mutations [120]. Functioning as a vital regulator of bacterial growth and differentiation, zinc ions actively contribute as cofactors in the synthesis of glycogen, lipids, and proteins [121]. While high concentrations of zinc inhibit bacterial growth [122]. An excess of zinc ions can specifically bind to bacterial proteins, resulting in their inactivation and denaturation. This process leads to the inhibition of bacterial growth. Among its various roles, zinc plays a crucial

part in the composition of proteins that facilitate osteoblast gene expression, proliferation, and differentiation. So adding an appropriate amount of zinc can stimulate new bone formation while also inhibiting bacterial growth [123]. Due to the active chemical nature of zinc, it can react with oxygen to form zinc oxide. Studies show that ZnO nanomaterials exhibit an excellent antibacterial effect against gram-positive bacteria [124]. ZnO has also received approval from the FDA for use in the human body [125]. Magnesium, as a new degradable antibacterial material, is one of the most promising medical metal materials. Yu *et al.* coated the surface of PEEK with a high-purity magnesium coating and found that the material's killing rate against *S. aureus* reached 99% due to the degradation of the magnesium coating [126]. However, when researchers use zinc ion-modified implants, they need to detect the concentration of zinc ions in the blood and the toxic side effects on different organs, because excessive zinc ions will have negative effects on living organisms. For example, animal experiments have shown that mice will develop pathological changes after oral administration of zinc oxide ($2.5\ g{\cdot}kg^{-1}$) [127]. Intratracheal perfusion of ZnO increased the number of neutrophils [128]. In addition, zinc oxide can increase ROS that damage the alveolar epithelium (Table 3).

4.2 Inorganic non-metallic antibacterial substances

Inorganic compounds, such as Si_3N_4 and titanium dioxide (TiO_2), also have unique antibacterial effects in PEEK implant. Tao *et al.* prepared nanometer TiO_2 thin films by hydrothermal method. Experiments show that the material has strong photocatalytic bactericidal performance [139]. Xian *et al.* grafted PDA onto PEEK to obtain PEEK–PDA–TiO_2 by liquid deposition of nano-TiO_2 coating [140]. This material possesses antibacterial properties due to the high aspect ratio of anatase-type TiO_2 and nanostructured surfaces that inhibit bacterial respiration and metabolism. In addition, Si_3N_4 is also an important antibacterial substance. Some researchers found that under the same bacterial group conditions, Si_3N_4 has the least number of bacteria on the surface of Si_3N_4 compared with Ti and PEEK. This materials has bacteriostatic ability [141]. These bacteria include but are not limited to *Staphylococcus epidermidis* [142], *S. aureus*, *E. coli*, *Pseudomonas aeruginosa*, *Enterococcus*. In view of the excellent antibacterial properties of Si_3N_4, Pezzotti *et al.* mixed Si_3N_4 with PEEK, and the volume content of Si_3N_4 was 15 vol%. It was found that PEEK–Si_3N_4 has inhibitory effect on gram-positive *S. epidermidis* [143].

Table 3: Material modification PEEK containing metallic elements

Material	Antibacterial material	Microorganisms	Results	Ref.
PEEK–Ag–CMC–BFP	Ag–CMC	*E. coli* *S. aureus*	*In vitro*: The material has inhibitory ability against *E. coli* and *S. aureus* due to the controlled release of Ag^+ by CMC	[129]
PEEK–SF–nAg–μCuO	Ag–CuO	*E. coli* *S. aureus*	At pH = 7.0, silk fibroin slowly released copper and silver ions in the material Common antibacterial mechanisms of silver and copper ions: bacterial membrane disruption, ROS production, protein inactivation	[130–133]
SS–PEEK/BG/MBGN–Ag/nSiO_2	Ag/nSiO_2	*S. carnosus* *E. coli*	Zone of inhibition: SS–PEEK/BG/MBGN–Ag/nSiO_2(RF40) > SS–PEEK/BG/MBGN Ag/nSiO_2(RF20) > SS–PEEK/BG/MBGN	[134]
PEEK/BG–Ag/Mn/MBGNs	Ag	*S. carnosus* *E. coli*	Zone of inhibition: PEEK/BG–Ag/Mn/MBGNs > PEEK/BG But quantitative evaluation of silver ion release is lacking	[135]
PEEK–$CuFe_2O_4$–GO	$CuFe_2O_4$/GO	*S. aureus* *E. coli*	The $CuFe_2O_4$/GO coating can kill more than 99.94% of *S. aureus* and 99.57% of *E. coli* PEEK–$CuFe_2O_4$/GO exhibited a circulating antibacterial rate of over 98% against both gram-positive and gram-negative bacteria	[136]
PEEK–PDA–Mn–Cu	Cu^{2+}	*E. coli* *S. aureus*	The antibacterial rate of PEEK–PDA–Mn/Cu against *E. coli* was 92.8%, and that against *S. aureus* was 91.5%	[137]
PEEK–nZnO	nZnO	*E. coli* *S. aureus*	Antibacteria: PEEK–nZnO (7.5 wt%) > PEEK–nZnO (5.0 wt%) > PEEK–nZnO (2.5 wt%) > PEEK–nZnO (1.0 wt%)	[138]

4.3 Organic antibacterial substances

Organic antimicrobials can also be synthesized on PEEK to provide antimicrobial properties. Organic bacterial antibacterial agents include antibiotics, antimicrobial peptides, and active ingredients of traditional Chinese medicine (Table 4).

4.3.1 Antibiotic

Many dental surgeries nowadays incorporate oral or intravenous antibiotics, which aid in mitigating issues related to bacterial infections [163]. However, it is important to note that oral or intravenous antibiotics have a delayed onset of action, and they carry the possibility of adverse reactions, including antibiotic resistance and circulatory collapse [164]. Therefore, the synergistic use of antibiotics and PEEK can directly manage bacterial infections. For example, Lauren *et al.* designed a cage with an antibiotic reservoir using PEEK material. The antibiotic reservoir is sealed by a polylactic acid (PLA) microbubble membrane [165]. PLA is a new type of biodegradable material. It has the function of carrying drugs and adsorbing ions. The PLA microbubble structure can be disrupted by ultrasound radiation, which allows the slow release of antibiotics from the orthopedic device. When the ultrasonic parameters were set as pulse repetition frequency of 6.4 kHz and acoustic output power of 100% (3.41 MPa), the antibacterial effect was the best [166]. Similarly, scientists can add different drugs to the device to control different types of infections, depending on the clinician's medical needs. The design of this orthopedic device can provide ideas for the development of antibacterial properties of oral implants. Some researchers synthesized Van-GNPs/PEEK with an antibacterial effect using low temperature argon plasma, chemical deposition, and PDA drug loading techniques. Van-GNP is a vancomycin gel nanoparticle prepared in the laboratory, characterized by the slow release of vancomycin. Vancomycin is a narrow-spectrum antibiotic effective against gram-positive bacteria. It can reduce the permeability of cell membrane and affect the replication of bacterial genetic material [167]. Gao *et al.* synthesized moxifloxacin hydrochloride (MOX) and osteogenic growth peptide (OGP) on a porous sulfonated PEEK (SPEEK) surface coated with PDA. The new material SPEEK–PDA–MOX/OGP has osteogenic effect while resisting infection [168]. The antibacterial properties of the material are mainly determined by MOX. MOX is a quinolone antibiotic with good broad-spectrum antibacterial activity and could prevent osteomyelitis. MOX inhibits bacterial DNA gyrase and topoisomerase IV, which in turn prevents bacterial DNA replication, which results in bacterial growth inhibition and death. This property can lead to rapid bacterial death while fighting antibiotic resistance. Xu *et al.* utilizes a layer-by-layer (LBL) deposition technique to introduce gentamicin (GS) and phosphate (CAP) into the PEEK material. Experiments have shown that the materials (PEEK/CAP-GS*6) prepared by six LBL cycles have favorable antibacterial ability [169]. Wang *et al.* synthesized PEEK modified with dexamethasone and minocycline loaded liposome, and the results showed that PEEK–Dex/Mino had well stability and cytocompatibility, as well as antibacterial properties [170]. Minocycline can bind to specific ribosomal subunits, which interferes with the association of bacterial ribosomes and tRNAs. This mechanism inhibits bacterial protein synthesis, making PEEK–Dex/Mino antibacterial [171]. A layer of hydroxyapatite coating (HA) about 200–760 nm was formed on PEEK material surface by ultrasonic coating technology, and the nano-hydroxyapatite (Go-HAP) coating was loaded with the antibiotic cephalosporin (CEF) at the concentration of 1 $mg{\cdot}cm^{-2}$. The results showed that PEEK–HAP1–CEF had a suitable antibacterial effect on *S. aureus* [172]. The antibacterial activity of the material is determined by the pore size of Go-HAP. The larger the pore size is, the larger the drug load is and the better the antibacterial activity is. Sang *et al.* embedded nano-carbonate-dopamine ($SrCO_3$/PDA) into a SPEEK with a microporous structure, combining GS–silk protein coating (GS/Silk) into the material surface [173]. This synthetic material has strong antibacterial properties both *in vitro* and *in vivo* because silk fibroin controls the slow release of GS [174]. And GS can inhibit gram-positive and gram-negative bacteria [175].

4.3.2 Antimicrobial peptide

Antibacterial peptides (AMPs) are natural antibacterial substances that currently have broad-spectrum resistance to bacteria [176]. AMPs can destroy multiple targets of pathogens, so it is less likely to develop bacterial resistance than antibiotics [177]. It can disrupt bacterial cell membranes at multiple sites or interfere with their protein synthesis. Li *et al.* synthesized OGP and AMP onto PEEK surface. This material (PEEK–OGP–AMP) has the function of inhibiting bacterial growth [178]. AMPs can attack pathogen cell membranes, making membrane proteins structurally abnormal, hindering cellular respiration and cell wall synthesis, which leads to bacterial death [179]. Yuan *et al.* synthesized the mouse beta-defensin-14 (MBD-14) onto a SPEEK surface. MBD-14 has broad-spectrum activity against multidrug-resistant bacteria and gram-positive and gram-negative bacteria, So SPEEK–MBD-14 has a durable

Table 4: Inorganic and organic antibacterial substances modified PEEK materials

Material	Antibacterial material	Microorganisms	Results	Ref.
PEEK–PDA–TiO_2	TiO_2	*S. aureus* *S. mutans*	Bacterial adhesion number: PEEK–PDA–TiO_2(12 h) < PEEK–PDA < PEEK The antibacterial rate of PEEK–PDA–TiO_2 against *S. aureus* is about 90% and against *S. mutans* is about 82%	[144]
PEEK–Si_3N_4	Si_3N_4	*S. epidermidis*	Antibacterial: PEEK–Si_3N_4 > PEEK; Si_3N_4 > PEEK	[145–148]
PEEK–Van-GNPs	Van	*S. aureus* *S. mutans*	The closer to Van-GNPs/PEEK, the higher the concentration of Van, the stronger the bactericidal effect	[149,150]
SPEEK–PDA–MOX–OGP	MOX	*S. aureus*	MOX inhibits *S. aureus* DNA synthase	[151]
PEEK–CAP-GS	GS	*S. aureus* *E. coli*	The number of LBL cycles on PEEK/CAP-GS is not significant On the sixth day, PEEK/CAP-GS*3 and PEEK/CAP-GS*6 lost antibacterial properties On the seventh day, PEEK/CAP-GS*9 lost antibacterial properties	[152]
PEEK–Dex/Mino lipo	Mino	*S. mutans* *P. gingivalis*	Bacterial colony count: PEEK–Dex/Mino lipo (2 ± 1) < PEEK (77 ± 44) The antibacterial rate of PEEK–Dex/Mino lipo against *S. mutans* is about 97.4%	[153]
PEEK–HAP–Cef	Cef	*S. aureus*	Antibacterial ability: PEEK–HAP–Cef > PEEK–HAP > PEEK Inhibition zone: after 24 h, the area of the PEEK–HAP–Cef antibacterial circle was 45.0 mm ± 2.0 mm	[154]
SPEEK–Silk/GSPDA/$SrCO_3$	Silk/GS	*S. aureus* *E. coli*	Antibacterial ability: SPEEK–GS/Silk–$SrCO_3$/PDA > SPEEK The number of adherent bacteria on SPEEK–GS/Silk–$SrCO_3$/PDA material was less than 102, which had obvious inhibitory effect on bacteria	[155]
SPEEK–MBD-14	MBD-14	*S. aureus* *P. aeruginosa*	Due to the presence of MBD-14, SPEEK–MBD-14 is approximately 100% antimicrobial against *S. aureus* and *P. aeruginosa*. The concentration of MBD-14 increased, and the antibacterial effect was enhanced	[156]
PEEK–OGP–AMP	AMP	*S. aureus* *E. coli*	PEEK–A_2O_2 can provide very good antibacterial efficiency (96%). A_2O_2 represents the material ratio of OGP and AMP	[157]
SPEEK–SA(CGA) –BFP	CGA	*S. aureus* *E. coli*	The degradation of hydrogel lead the release of CGA, which makes the new material have a good antibacterial effect on gram-positive bacteria and gram-negative bacteria	[158]
PEEK–nMCS–CR–GS	CR	*S. aureus* *E. coli*	Due to the addition of CR, the reduction rate of PEEK–nMCS–CR–GS against *S. aureus* was 99.62%, and the reduction rate against *E. coli* was 98.59%	[159]
SPEEK–ZrO_2–Cur	Cur	*Streptococcus oralis-2696*	Anti-bacterial test: SPEK–NH–ZrO_2–Cur (8 ± 1 mm) > SPEK–NH_2–ZrO_2 (7.5 ± 1 mm) > SPEK (6.5 ± 0.5 mm)	[160]
SPEEK–Ost–Ber	Ber	*S. aureus* *S. epidermidis*	The number of bacteria adhering to this material was low compared to the control group. SPEEK–Ost–Ber has good bacteriostatic effect on *S. aureus* and *S. epidermidis* in suspension	[161]
316SS–PEEK/BG–chitosan/gelatin/Ag–Mn	Mn/Ag chitosan	*S. carnosus* *E. coli*	Bacterial inhibition zone: 316L–PEEK/BG–chitosan/gelatin/Ag–Mn > 316L–PEEK/BG	[162]

antibacterial effect [180]. This durable antibacterial property may be related to the covalent immobilization of MBD-14 with SPEEK and the contact absorption of MBD-14 on the material.

4.3.3 Coating herbal extract antibacterial agent

In recent years, the active ingredients in herbal medicine extracts have also become a research hotspot of antibacterial organic compounds. Since this type of organic matter is extracted from natural herbs, it has fewer side effects on the human body when it is antibacterial [181]. In addition, these antibacterial ingredients have significant antibacterial effects, like as butyrate and chlorogenic acid (CGA) [182]. The PEEK modified by these antibacterial materials has obtained excellent antibacterial properties. CGA, also known as caffeic acid, is an ester compound extracted from natural plants such as *Phyllostachys edulis* and honeysuckle. It is formed by condensation of caffeic acid, L-quinic acid, and the third hydroxyl group. It has antibacterial and antiviral properties [183]. He *et al.* constructed a CGA/grafted peptide (BFP) hydrogel system on a SPEEK. Due to the excellent antibacterial effect of CGA, the modified PEEK has inhibitory effects on both gram-positive and gram-negative bacteria [184]. Curcumin (Cur) is a low molecular weight polyphenolic compound extracted from turmeric with low toxicity to human cells. It also has antibacterial and anti-inflammatory effects. Zo *et al.* introduced a nano-porous magnesium calcium silicate (n-MCS) coating on the surface of PEEK, and then loaded CR and genistein (GS) on it to synthesize PEEK–nMCS–CR–GS [185]. Ekambaram *et al.* used electrospinning technology and amination reaction technology to composite Cur and zirconia (ZrO_2) into SPEEK. Due to the addition of Cur, the laboratory found that SPEEK–NH_2–ZrO_2–Cur has an antibacterial effect on *Streptococcus oralis*-2696 [186]. Berberine, an extract from the Chinese herb Coptis chinensis, can interfere with bacterial DNA replication and protein synthesis, which can inhibit staphylococci. Sang *et al.* embedded nanoparticles (Ost) on SPEEK, and then bound a silk fibroin-berberine coating (Ber) on the surface of the material. But the drug is highly soluble in water. However, silk fibroin, which has abundant carboxyl groups, covalently adsorbs with berberine, and increases the loading of berberine on the material, which can control the slow release of berberine. This material prevents bacteria from sticking and has a killing effect on the surrounding suspended bacteria [187].

5 Modification of PEEK for increased osseointegration activity

The modification methods to improve the bone integration ability of PEEK mainly include surface modification and blending modification. Surface modification entails altering a material's surface or applying a protective or functional coating without affecting the material's chemical composition. PEEK surface modification methods primarily involve physical treatment, bioactive material coating, and chemical treatment. Blending modification refers to the mixing of different materials together to form a PEEK composites. These techniques enhance the biological compatibility of PEEK while preserving its original mechanical properties, facilitating seamless integration with natural bone tissue (Figure 7).

5.1 Physical treatment

Physical treatment modification refers to the use of heat, force, light, electricity, and other means to change the shape, structure, and properties of the material surface. The physical methods currently used in the modification of PEEK include accelerated neutral atomic beam (ANAB) technology, ion beam-assisted deposition (IBAD), plasma, and nano-structured PEEK surfaces (Figure 8).

5.1.1 ANAB modification

ANAB technology is a widely accepted accelerated particle beam technology, which has been used as a nano-scale surface modification tool in the fields of implantable medical devices with rapid and economical characteristics [188]. ANAB not only induces amorphous atomic layer formation on the material's surface but also alters its surface morphology. Recent research suggests that ANAB can boost the biological activity of biomaterial surfaces and reduce surface roughness without affecting the overall mechanical properties. Khoury *et al.* found that ANAB processing improves UHMWPE wear resistance by aligning its surface energy with key body proteins, reducing bacterial adhesion by mucins, casein, and lubricating proteins. Ajami *et al.* demonstrated that ANAB-treated PEEK surfaces enhance cell attachment and improve biocompatibility. Cells show

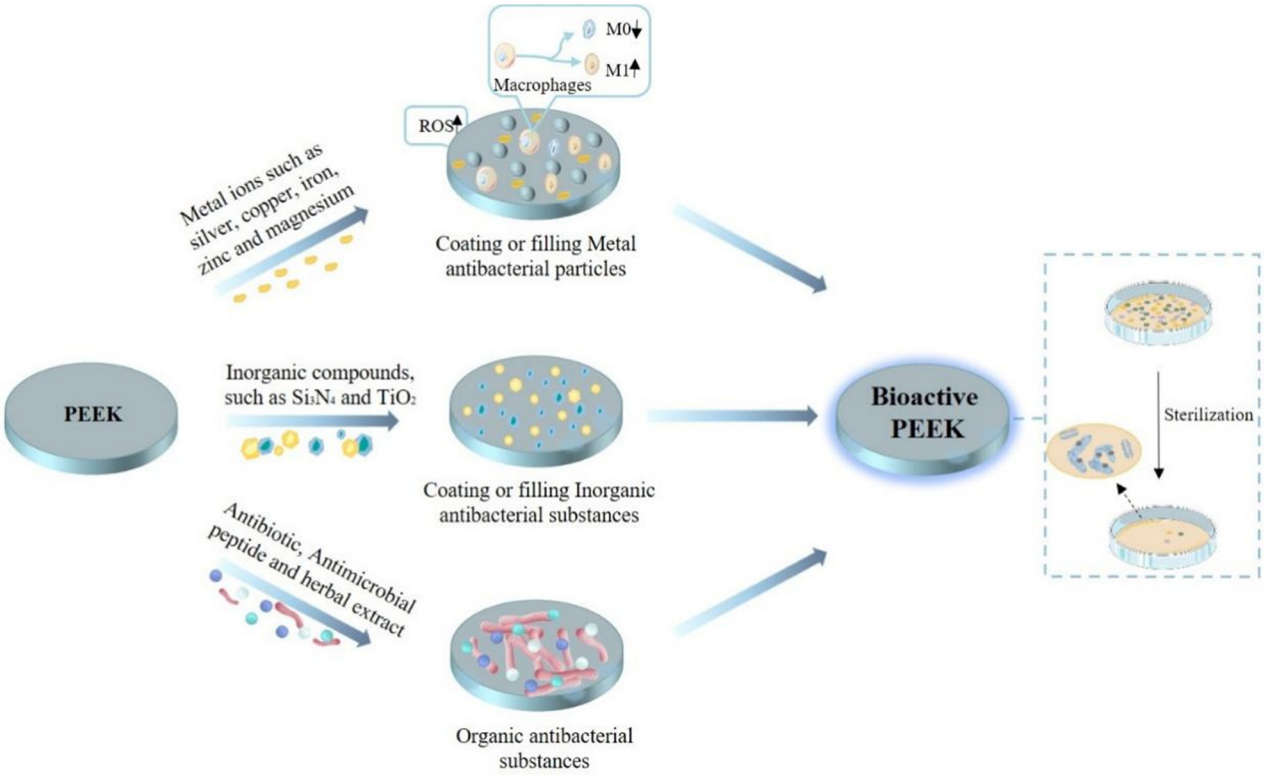

Figure 7: Strategies for increasing the antibacterial activity of PEEK. ROS: reactive oxygen species.

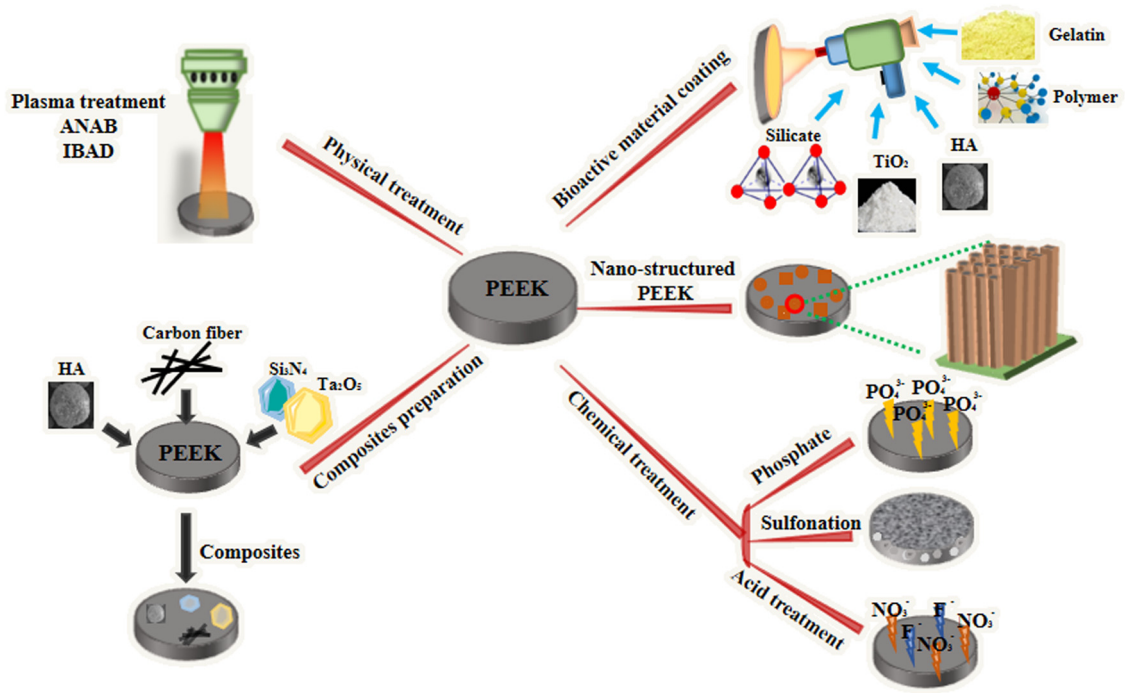

Figure 8: Osteogenic modification method of PEEK.

enhanced metabolic activity and growth on ANAB-treated PEEK, indicating its promise for improving bone integration in PEEK implants [189].

5.1.2 IBAD modification

IBAD is a thin film deposition technique that creates denser specialized thin films, providing superior mechanical strength, environmental stability, moisture resistance, and weather resistance compared to conventional methods. In a study by John *et al.* IBAD was used to coat a cylindrical PEEK substrate with HA/YSZ at room temperature [190]. The study's tensile test results suggest that increasing substrate roughness can enhance coating strength. When combined with IBAD, this has the potential to optimize bioactive HA/YSZ coatings for promoting bone growth and integration in implantable PEEK biomaterials. *In vitro* research by John and colleagues has shown that crystalline HA/YSZ coatings promote osteoblast differentiation, expediting osteoblastic maturation and bone growth [191]. Specifically, the coating after microwave and autoclave heat treatment exhibited superior biological activity.

5.1.3 Plasma modification

Plasma modification is a simple and effective surface modification strategy. Ionizing gas bombardment in a confined space can enhance PEEK surface functional groups, create surface roughness, and enhance cell adhesion and PEEK's biological activity. Štefanikova *et al.* found that plasma-treated PEEK, when compared to untreated PEEK, displayed increased water contact hysteresis and greater spatial heterogeneity [192]. The biological activity of plasma-modified materials is related to the type of plasma. Liu *et al.* found that compared with the unprocessed PEEK, the PEEK-N (N_2 cold plasma treatment group) had the highest roughness and the strongest hydrophilicity. In addition, compared with the unprocessed PEEK, the osteogenic activity of the experimental group was significantly improved. In the experimental groups, PEEK-N had the best osteogenic activity and PEEK-A (Ar cold plasma treatment group) had the weakest osteogenic activity. N_2 cold plasma treatment is the most suitable modification method for PEEK in implantable medical devices [193]. Fu *et al.* treated standard PEEK with hydrogen and oxygen plasma, and tested the surface roughness, surface contact angle, surface microhardness, surface crystallinity, and human osteoblast coverage area of each group. The results showed that the low-pressure plasma treatment evaluated in the experiment had significant effects on the hydrophilicity, crystallinity, and microhardness of PEEK surface. In addition, the adhesion and proliferation rate of human osteoblasts on plasma treated PEEK surface was significantly increased, and further research results showed that plasma treatment with a hydrogen to oxygen ratio of 2/1 was effective in all experimental groups [194]. Wang *et al.* used a combination process of sulfonation and argon plasma treatment to combine polar functional groups and layered micro/nano-morphology on PEEK surface, which improved the viability and alkaline phosphatase (ALP) activity of MG-63 cells, promoted the formation of calcium nodules and the expression of osteogenic genes in MG-63 cells [195]. Yu *et al.* prepared CF-reinforced PEEK (CFR–PEEK) composite material by plasma modification technology, and modified it with amino group. The evaluation results of CFR–PEEK surface characterization are as follows: the surface of CFR–PEEK successfully combined with amino groups has significantly improved hydrophilicity, and the results of *in vitro* experiments show that the amino-modified CPEEK has enhanced biological activity and osteogenic properties [196]. Lu *et al.* prepared the calcium-containing PEEK surface by calcium plasma immersion ion implantation method. The results confirmed that modified layers with different calcium contents were formed on the PEEK surface. Compared with the untreated PEEK surface, the hydrophobicity of the Ca-treated surface increased. The adhesion, proliferation, and bone differentiation of bone mesenchymal stem cells (BMSCs) treated with Ca-PIII were improved [197]. Zhang *et al.* successfully constructed an acrylic (AA) polymer coating supported by zinc ions (Zn^{2+}) on the surface of PEEK (PEEK–AA–Zn) using a combination of plasma-induced graft polymerization and chemical immersion. The AA coating effectively loaded and released Zn^{2+}. *In vitro* cell experiments showed that Zn^{2+} released by PEEK–AA–Zn promoted cell proliferation and increased the expression levels of osteocalcin, ALP, and bone sialoprotein genes. It is obvious that the combination of grafting polymerization and ion incorporation makes PEEK have good osteogenic properties [198].

5.1.4 Nano-structured PEEK modification

As a PEEK modification technique, nano-modification has the advantage of preventing debonding. The nanoparticles can form a larger interface, enhancing particle–matrix interaction. There are various nano-morphologies, including grooves, columns, and pores. The nano-porous surface can promote cell adhesion, diffusion, and differentiation, and improve the osteogenic ability. Johansson *et al.* evaluated

a unique nano-modified PEEK's relationship between surface and bone integration by conducting a rabbit experiment. The results demonstrated that incorporating a nanoscale hydroxyapatite coating on the PEEK surface significantly enhanced removal torque and improved biocompatibility, which is advantageous for bone integration [199]. Lu *et al.* introduced a unique micro/nano-structure mixed with zinc into CFR–PEEK surfaces. *In vitro* cell experiments showed that the adhesion, proliferation, and bone differentiation of mouse osteoblasts (MC3T3E1) and rat BMSCs were enhanced on the structural surface. It was proved that the addition of zinc and the introduction of multilayer structure enhanced the specific biological properties of CFR–PEEK surface, and further expanded the application of CFR–PEEK in dental implants [200].

5.2 Bioactive material coating

PEEK has the advantages of high melting point, good fatigue resistance, good wear resistance, non-toxic, and suitable elastic modulus, so it can be used as a potential substitute for metal implant materials in dental applications [201]. Nevertheless, this material suffers from limited bioactivity. One solution involves surface-coating the implant with bioactive substances, including hyaluronic acid, Ti, TiO_2, silicate, magnesium phosphate, calcium phosphate, gelatin, and proteins. The incorporation of these bioactive coatings significantly boosts the surface osteogenic activity of PEEK.

Deng *et al.* made use of the unique biological activity of n-TiO_2 and combined the PEEK polymer with n-TiO_2 to prepare n-TiO_2/PEEK nanocomposites. Both cellular experiment results and *in vivo* study results showed that n-TiO_2 significantly improved the biological activity of PEEK, especially when it had a rough composite surface [202]. In an experimental study to explore the effect of aging on the fracture characteristics of polyether ketone crowns, Lu *et al.* found that adding 20% TiO_2 particles to PEEK crowns increased the fracture load under compression test compared to PEEK crowns without TiO_2, the underlying mechanism of which will be further investigated [203]. Shimizu *et al.* established a canine cervical anterior fusion model for *in vivo* experimental study. In the experiment, PEEK was coated with sol–gel-derived TiO_2 coating. The results showed that bioactive PEEK implants coated with TiO_2 showed better fusion rate and osseointegration [204]. Gelatin is an irreversibly hydrolyzed form of collagen extracted from animal skin, bone, or cartilage, mainly found in bone and skin. Gelatin has the advantages of good biocompatibility, adhesion, chemical stability, biodegradability, and belongs to non-specific biodegradable biomaterials. In recent years, gelatin has been widely used in biomedicine. Wu *et al.* used phosphorylated gelatin to support covalent coating of bone morphogenetic protein 2 (BMP-2) to enhance bioactive cells. The experimental results showed that surface modification of microporous PEEK with phosphorylated gelatin could significantly promote cell adhesion and proliferation [205]. Zhang *et al.* added glutaraldehyde and gelatin solution to the surface of PDA-modified PEEK, and chemically combined gelatin hydrogel with PEEK. Cell experiments showed that the continuous release of BMP-2 by modified PEEK could promote the osteogenic differentiation of BMSCs [206]. HA is the main component of vertebrate bones and teeth. HAP has excellent biocompatibility and bioactivity [207]. Researchers not only enhance the bioactivity of PEEK by preparing PEEK/HAP composites, but also enhance the bioactivity of PEEK by preparing degradable hybrid coatings on its surface [208]. Studies have shown that PEEK/HA composites significantly improve cell adhesion, proliferation, osteogenic differentiation, and mineralization [209]. Almasi *et al.* applied a friction stir processing technique to synthesize HA/PEEK surface nanocomposites by depositing HA onto PEEK surface. Compared with the original PEEK, the synthesized HA/PEEK material formed bone-like hydroxyapatite on its surface in SBF solution, which showed better surface hydrophilicity and enhanced the biological activity of PEEK. Yak *et al.* studied a porous PEEK scaffold with a stable HA coating. The highly porous structure of PEEK/HA scaffold and the hyaluronic acid coating promoted bone integration and biomineralization [210]. Biomaterials based on silicates have received increasing attention in the treatment of bone defects and have been used in a variety of biomedical applications. Wen *et al.* introduced bioactive silicate coating on PEEK surface to improve the bone integration of PEEK. This study has shown that silicon-coated PEEK has good osteogenic effect and can effectively release silicon *in vitro* and *in vivo* [211].

5.3 Chemical treatment

Chemical modification refers to change in the physical and chemical properties of polymers through chemical reactions. The chemical methods currently used in the modification of PEEK include sulfonation modification, phosphate modification, and acid treatment.

5.3.1 Sulfonation modification

Many techniques in addition to gaseous sulfur trioxide (SO_3) can be used to introduce sulfonic groups onto the surface of PEEK [212]. For example, sulfuric acid treatment [213], ultraviolet-initiated graft polymerization, and so on [214]. Sulfonation modification refers to introduce $-SO_3H$ and sulfonyl group into PEEK. Due to the inherent chemical inertness of PEEK, it is both critical and difficult to prepare the required porous structures on its surface to enhance biological function. By sulfonation modification, $-SO_3H$ was introduced to bind to the PEEK surface and form a porous structure to maintain excellent mechanical properties. The results of several studies suggest that controlled sulfonation by gaseous SO_3 would be an effective strategy to improve the bone integration of PEEK implants by adjusting the microstructure and chemical composition while maintaining excellent mechanical properties [215]. Finally, the samples were washed with deionized water at room temperature for 5 min, and the samples were left overnight to dry at room temperature [216]. A porous network structure formed on all the sulfonated samples. With the increase in sulfonation time and concentration, the porous structures became more obvious. A surface porous structure was produced on the surface of PEEK materials due to sulfonation with SO_3. Then the morphology of porous structure, chemical characteristics, wettability, protein adsorption capacity, mineralization behavior, and mechanical property of the different SPEEK samples were systematically evaluated [217]. Furthermore, in order to evaluate osseointegration properties of the modified PEEK, a series of *in vitro* experiments were performed including cell adhesion, spreading, proliferation as well as extracellular matrix secretion [218].

5.3.2 Phosphate modification

Phosphorylation refers to the addition of phosphoric acid groups to PEEK materials by various chemical means, which can increase the biological activity and mechanical properties of the surface of the material [219]. The PEEK implants surface modified with phosphoric acid groups are outstanding for the pro-osteogenic capability. Many methods can be used to achieve the phosphate modification of PEEK [220]. Ultraviolet-initiated graft polymerization [221], tailored silanization layers technique, and PDA-mediated method all can be used to introduce phosphoric acid groups on PEEK. Petrovic *et al.* combined PEEK and b-TCP as alternative materials for composite applications. Normal human osteoblasts were inoculated on polymer disks, and cell viability and proliferation were evaluated after 24, 72, and 120 h culture by WST-1 assay. The results show that the mechanical properties of the composite partly match the mechanical properties of human bone. The proliferation rate of osteoblasts on b-TCP–PEEK was lower than that of pure PEEK. Based on these findings, b-TCP–PEEK is considered to have inhibitory effects on osteoblast growth *in vitro* [222]. Sunarso *et al.* proposed a strategy of combined phosphate and calcium surface-functionalization, in which ozone-gas treatment and wet chemistry were used for introduction of hydroxyl groups and modification of phosphate and/or calcium, respectively. Surface functionalization significantly elevated the surface hydrophilicity without changing the surface roughness or topography. Cell experiments showed that the activity of rat mesenchymal stem cells growing on modified PEEK was significantly increased. Furthermore, they successfully prepared phosphate and/or calcium surface functionalized PEEK through ozone and chemical treatment. This surface chemical functionalization is a promising technique for increasing the osseointegration capability of PEEK implants [223].

5.3.3 Other acid treatment

Acid treatment refers to form pores on the surface of PEEK implant using a mixed acid of sulfuric acid and nitric acid. This PEEK has high potential for use as a bone substitute that promotes bone formation [224]. Huo *et al.* simultaneously treated the surface modification of PEEK with hydrofluoric acid and nitric acid (AFN). The microstructure of the modified PEEK surface was observed under scanning electron microscope. The expression of cell adhesion, survival, and specific marker genes used for cultured rat bone marrow mesenchymal stem cells was measured. It was found that AFN treatment of PEEK could achieve better adhesion, diffusion, and proliferation of osteoblasts. In addition, the results show that PEEK–AFN bio-composite is cytocompatible after surface treatment of PEEK with hydrofluoric acid and nitric acid, and enhances bone formation and regulates macrophage polarization better than naked PEEK [225].

5.4 PEEK composites

Mixed modification of PEEK is another method to enhance the osteogenic activity of PEEK. The current mainstream addition methods are CF and hydroxyapatite. CF has already been widely used in some files because of its

high specific strength, high specific modulus, and excellent corrosion resistance. CFR–PEEK is often used as an orthopedic implant material due to its high shock resistance and thermostability [226]. Yet recently, some studies have shown that there is a challenge in CF-reinforced CF/PEEK composites due to non-polarity and poor wettability of CF between CF and PEEK. To exert the excellent mechanical properties and thermal stability of CFR–PEEK, the addition of bioactive nanofillers or surface modification may increase its biological activity. Below are examples of CFR–PEEK modification [227]. Yan *et al.* coated graphene onto the surface of CFR–PEEK. *In vitro* and *in vivo* experiments showed that the graphene-modified version of CFR–PEEK exhibited satisfactory cytocompatibility and promoted osteogenesis. Furthermore, Through Van Gieson staining, they also found that there are more new bones around graphene-modified CFR–PEEK implants than CFR–PEEK implants [228]. Deng *et al.* prepared a unique PEEK bioactive ternary composite, PEEK/n-HA/CF by a process of compounding, injection and then evaluated its mechanical properties and biological performances. The results showed that n-HA and CF was uniformly distributed in the PEEK matrix and PEEK/n-HA/CF increased hydrophilicity. Cell experiments demonstrated that modified PEEK promoted attachment and proliferation of cells. In addition, through analyzing the 3D micro-CT data, they also found that there was a greater formation of new bone around the PEEK/n-HA/CF [229].

HA has excellent biocompatibility and bioactivity, participating in body metabolic processes and accelerate bone healing. Recent studies have shown that the HA coating had a dense microstructure with no cracks or pores and showed better tensile and fatigue properties compared to conventional HA powders [230]. Feng *et al.* built a nano-sandwich construct which is composed of two-dimensional graphene nanosheets (GNSs) and one-dimensional CNTs to improve the biocompatibility of HAP–PEEK scaffolds for bone tissue engineering. They found that HAP–PEEK increased the effective contact area between the construct and matrix. Cell experiments showed that the cells attached and spread well on the surface of the scaffolds and the adhesion and proliferation ability were better than pure PEEK [231]. Huang *et al.* synthesized PEEK–HA composites consisting of GO, HAP *via* scalable extrusion and injection molding followed by laser machining. Incorporation of GO and HAP significantly increased bone growth and fusion. More importantly, they found that compared to the pure PEEK, the composites with macro-porous surface exhibit better cell viability and provided a better environment for bone growth [232].

6 Conclusions

Solving challenges of the weak mechanical properties, poor bone integration, and susceptibility to bacterial infection of PEEK implants are key problems in its application. Orthopedic implants not only need to resist long-term chemical erosion but also need to be able to resist friction, fatigue, shear force, and violence. Moreover, how to improve the antibacterial and osteogenic properties of PEEK while improving the mechanical properties is the future development direction of PEEK-based composites. There is still a lot of research on how to ensure the stability of antibacterial functionalized PEEK under different stresses and the uniform and effective release of antibacterial substances. Regarding osteogenic properties, the composites obtained by blending modification may be prone to crack propagation under external force due to the poor interfacial bonding strength between micron filler and PEEK matrix. Developing interface materials with strong affinity to both filler and PEEK matrix and selecting appropriate methods to process the required composite materials are the key tasks for the successful clinical transformation of PEEK.

3D bioprinting is likely to become the main technology for designing and manufacturing orthopedic implants in the future. Biological 3D printing technology provides a great possibility for accurately and conveniently constructing bionic human skeleton structure from macro to micro. The application of 3D printing technology makes it possible for PEEK's personalized medical treatment. Unfortunately, the accuracy of the current 3D printing technology makes it difficult to copy some nano-scale fine structures. At the same time, the innovation of high-temperature printing system and the exploration of suitable printing parameters will also have a revolutionary impact on the performance of PEEK and other implant materials. Further research and clinical trials are still needed for future innovation to release the untapped potential of PEEK implants and expand their application scope.

This article summarizes the research results of many scholars in recent years, introduces the methods of mechanical modification, antibacterial modification, and osteogenic modification of PEEK, and looks forward to the future research direction and problems to be further solved, which makes contributions to the modification and application of PEEK.

Acknowledgments: The authors would like to acknowledge the support of the Natural Science Foundation of Liaoning Province of China for paying the Article Processing Charges (APC) of this publication.

Funding information: This work was supported by the Medical Engineering Intersection Joint Funds of the Natural Science Foundation of Liaoning Province of China (2021-YGJC-18).

Author contributions: Conceptualization: Q.W., B.G., Z.L. (Zhimin Li), and H.S.; writing – original draft: M.C., Y.Y., and H.Z.; writing – review and editing and visualization: C.L., Y.Y., H.Z., and Z.L. (Zhanglong Li); supervision: C.L. and Y.Y. All authors have accepted responsibility for the entire content of this manuscript and approved its submission.

Conflict of interest: The authors state no conflict of interest.

References

[1] Luo, C., Y. Liu, B. Peng, M. Chen, Z. Liu, Z. Li, et al. PEEK for oral applications: recent advances in mechanical and adhesive properties. *Polymers*, Vol. 15, 2023, id. 386.

[2] Zhang, Y. and B. R. Lawn. Novel zirconia materials in dentistry. *Journal of Dental Research*, Vol. 97, 2018, pp. 140–147.

[3] Sailer, I., D. Karasan, A. Todorovic, M. Ligoutsikou, and B. E. Pjetursson. Prosthetic failures in dental implant therapy. *Periodontology 2000*, Vol. 88, 2022, pp. 130–144.

[4] Souza, J. C. M., M. B. Sordi, M. Kanazawa, S. Ravindran, B. Henriques, F. S. Silva, et al. Nano-scale modification of titanium implant surfaces to enhance osseointegration. *Acta Biomaterialia*, Vol. 94, 2019, pp. 112–131.

[5] Kaur, M. and K. Singh. Review on titanium and titanium based alloys as biomaterials for orthopaedic applications. *Materials Science and Engineering: C*, Vol. 102, 2019, pp. 844–862.

[6] Zol, S. M., M. S. Alauddin, Z. Said, M. I. Mohd Ghazali, L. Hao-Ern, D. A. Mohd Farid, et al. Description of poly(aryl-ether-ketone) materials (PAEKs), polyetheretherketone (PEEK) and polyether-ketoneketone (PEKK) for application as a dental material: a materials science review. *Polymers*, Vol. 15, 2023, id. 2170.

[7] Padhan, M., U. Marathe, and J. Bijwe. Tribology of poly(etherketone) composites based on nano-particles of solid lubricants. *Composites Part B: Engineering*, Vol. 201, 2020, id. 108323.

[8] Verma, S., N. Sharma, S. Kango, and S. Sharma. Developments of PEEK (polyetheretherketone) as a biomedical material: a focused review. *European Polymer Journal*, Vol. 147, 2021, id. 110295.

[9] Xu, Q., G. Wang, C. Xiang, X. Cong, X. Gai, S. Zhang, et al. Preparation of a novel poly (ether ether ketone) nonwoven filter and its application in harsh conditions for dust removal. *Separation and Purification Technology*, Vol. 253, 2020, id. 117555.

[10] Zhu, Y., Z. Cao, Y. Peng, L. Hu, T. Guney, and B. Tang. Facile surface modification method for synergistically enhancing the biocompatibility and bioactivity of poly(ether ether ketone) that induced osteodifferentiation. *ACS Applied Materials and Interfaces*, Vol. 11, 2019, pp. 27503–27511.

[11] Cao, N., Y. Sun, J. Wang, H. Zhang, J. Pang, and Z. Jiang. Strong acid- and solvent-resistant polyether ether ketone separation membranes with adjustable pores. *Chemical Engineering Journal*, Vol. 386, 2020, id. 124086.

[12] Han, X., W. Gao, Z. Zhou, S. Yang, J. Wang, R. Shi, et al. Application of biomolecules modification strategies on PEEK and its composites for osteogenesis and antibacterial properties. *Colloids and Surfaces B: Biointerfaces*, Vol. 215, 2022, id. 112492.

[13] Wang, X., J. Guo, J. Wen, X. Zhang, L. Cao, D. Zeng, et al. Novel vascular strategies on polyetheretherketone modification in promoting osseointegration in ovariectomized rats. *Materials and Design*, Vol. 202, 2021, id. 109526.

[14] Di Maggio, B., P. Sessa, P. Mantelli, P. Maniscalco, F. Rivera, G. M. Calori, et al. PEEK radiolucent plate for distal radius fractures: multicentre clinical results at 12 months follow up. *Injury*, Vol. 48, 2017, pp. S34–S38.

[15] Sikder, P., J. A. Ferreira, E. A. Fakhrabadi, K. Z. Kantorski, M. W. Liberatore, M. C. Bottino, et al. Bioactive amorphous magnesium phosphate-polyetheretherketone composite filaments for 3D printing. *Dental Materials*, Vol. 36, 2020, pp. 865–883.

[16] Wang, B., M. Huang, P. Dang, J. Xie, X. Zhang, and X. Yan. PEEK in fixed dental prostheses: application and adhesion improvement. *Polymers*, Vol. 14, 2022, id. 2323.

[17] Kumar, N., K. G. Lopez, S. Alathur Ramakrishnan, J. T. P. D. Hallinan, J. Y. H. Fuh, N. Pandita, et al. Evolution of materials for implants in metastatic spine disease till date – have we found an ideal material? *Radiotherapy and Oncology*, Vol. 163, 2021, pp. 93–104.

[18] Wang, Z., Y. Wang, J. Yan, K. Zhang, F. Lin, L. Xiang, et al. Pharmaceutical electrospinning and 3D printing scaffold design for bone regeneration. *Advanced Drug Delivery Reviews*, Vol. 174, 2021, pp. 504–534.

[19] Fabris, D., J. P. A. Moura, M. C. Fredel, J. C. M. Souza, F. S. Silva, and B. Henriques. Biomechanical analyses of one-piece dental implants composed of titanium, zirconia, PEEK, CFR-PEEK, or GFR-PEEK: stresses, strains, and bone remodeling prediction by the finite element method. *Journal of Biomedical Materials Research*, Vol. 110, 2022, pp. 79–88.

[20] Kurtz, S. M. and J. N. Devine. PEEK biomaterials in trauma, orthopedic, and spinal implants. *Biomaterials*, Vol. 28, 2007, pp. 4845–4869.

[21] Lee, W.-T., J.-Y. Koak, Y.-J. Lim, S.-K. Kim, H.-B. Kwon, and M.-J. Kim. Stress shielding and fatigue limits of poly-ether-ether-ketone dental implants. *Journal of Biomedical Materials Research*, Vol. 100B, 2012, pp. 1044–1052.

[22] Fabris, D., J. P. A. Moura, M. C. Fredel, J. C. M. Souza, F. S. Silva, and B. Henriques. Biomechanical analyses of one-piece dental implants composed of titanium, zirconia, PEEK, CFR-PEEK, or GFR-PEEK: stresses, strains, and bone remodeling prediction by the finite element method. *Journal of Biomedical Materials Research*, Vol. 110, 2022, pp. 79–88.

[23] Tsakiris, V., C. Tardei, and F. M. Clicinschi. Biodegradable Mg alloys for orthopedic implants – a review. *Journal of Magnesium and Alloys*, Vol. 9, 2021, pp. 1884–1905.

[24] Wang, X., B. Ning, and X. Pei. Tantalum and its derivatives in orthopedic and dental implants: osteogenesis and antibacterial properties. *Colloids and Surfaces B: Biointerfaces*, Vol. 208, 2021, id. 112055.

[25] Adhikari, S., T. Mukhopadhyay, A. Shaw, and N. P. Lavery. Apparent negative values of Young's moduli of lattice materials under dynamic conditions. *International Journal of Engineering Science*, Vol. 150, 2020, id. 103231.

[26] Kedziora, S., T. Decker, E. Museyibov, J. Morbach, S. Hohmann, A. Huwer, et al. Strength properties of 316L and 17-4 PH stainless

steel produced with additive manufacturing. *Materials*, Vol. 15, 2022, id. 6278.
[27] Han, X., T. Sawada, C. Schille, E. Schweizer, L. Scheideler, J. Geis-Gerstorfer, et al. Comparative analysis of mechanical properties and metal-ceramic bond strength of Co–Cr dental alloy fabricated by different manufacturing processes. *Materials*, Vol. 11, 2018, id. 1801.
[28] Hanawa, T. Zirconia versus titanium in dentistry: a review. *Journal of Dental Research*, Vol. 39, 2020, pp. 24–36.
[29] Ji, Y., H. Zhang, J. Ru, F. Wang, M. Xu, Q. Zhou, et al. Creating micro-submicro structure and grafting hydroxyl group on PEEK by femtosecond laser and hydroxylation to synergistically activate cellular response. *Materials and Design*, Vol. 199, 2021, id. 109413.
[30] Rea, M., S. Ricci, P. Ghensi, N. P. Lang, D. Botticelli, and C. Soldini. Marginal healing using polyetheretherketone as healing abutments: an experimental study in dogs. *Clinical Oral Implants*, Vol. 28, 2017, pp. 46–50.
[31] Wang, L., H. He, X. Yang, Y. Zhang, S. Xiong, C. Wang, et al. Bimetallic ions regulated PEEK of bone implantation for antibacterial and osteogenic activities. *Materials Today Advances*, Vol. 12, 2021, id. 100162.
[32] Long, E. G., M. Buluk, M. B. Gallagher, J. M. Schneider, and J. L. Brown. Human mesenchymal stem cell morphology, migration, and differentiation on micro and nano-textured titanium. *Bioactive Materials*, Vol. 4, 2019, pp. 249–255.
[33] Wu, D., Q. Miao, Z. Dai, F. Niu, and G. Ma. Effect of voids and crystallinity on the interlaminar shear strength of in-situ manufactured CF/PEEK laminates using repass treatment. *Composites Science and Technology*, Vol. 224, 2022, id. 109448.
[34] Miao, Q., Z. Dai, G. Ma, F. Niu, and D. Wu. CF/PEEK interleaved laminates with PEEK film interleaving manufactured by laser-assisted forming: microstructure and interlaminar shear strength. *Composites Part A: Applied Science and Manufacturing*, Vol. 172, 2023, id. 107592.
[35] Xu, W., S. Jambhulkar, Y. Zhu, D. Ravichandran, M. Kakarla, B. Vernon, et al. 3D printing for polymer/particle-based processing: a review. *Composites Part B: Engineering*, Vol. 223, 2021, id. 109102.
[36] Guo, Z., J. Xie, J. Yang, J. Fu, and P. Zhao. Rapid mold temperature rising method for PEEK microcellular injection molding based on induction heating. *Journal of Materials Research and Technology*, Vol. 26, 2023, pp. 3285–3300.
[37] Guo, Z., J. Xie, J. Yang, J. Fu, and P. Zhao. Rapid mold temperature rising method for PEEK microcellular injection molding based on induction heating. *Journal of Materials Research and Technology*, Vol. 26, 2023, pp. 3285–3300.
[38] Chen, Z., Y. Chen, J. Ding, and L. Yu. Blending strategy to modify PEEK-based orthopedic implants. *Composites Part B: Engineering*, Vol. 250, 2023, id. 110427.
[39] Siddiq, A. and A. R. Kennedy. Compression moulding and injection over moulding of porous PEEK components. *Journal of the Mechanical Behavior of Biomedical Materials*, Vol. 111, 2020, id. 103996.
[40] Van De Werken, N., P. Koirala, J. Ghorbani, D. Doyle, and M. Tehrani. Investigating the hot isostatic pressing of an additively manufactured continuous carbon fiber reinforced PEEK composite. *Additive Manufacturing*, Vol. 37, 2021, id. 101634.
[41] Lai, J., C. Wang, and M. Wang. 3D printing in biomedical engineering: processes, materials, and applications. *Applied Physics Reviews*, Vol. 8, 2021, id. 021322.
[42] Siddiq, A. and A. R. Kennedy. Compression moulding and injection over moulding of porous PEEK components. *Journal of the Mechanical Behavior of Biomedical Materials*, Vol. 111, 2020, id. 103996.
[43] Van De Werken, N., P. Koirala, J. Ghorbani, D. Doyle, and M. Tehrani. Investigating the hot isostatic pressing of an additively manufactured continuous carbon fiber reinforced PEEK composite. *Additive Manufacturing*, Vol. 37, 2021, id. 101634.
[44] Han, J., J. Tong, X. Tian, L. Xia, and D. Ma. Thermal simulation and warping deformation experimental study of PEEK in material extrusion. *Macro Theory and Simulations*, Vol. 30, 2021, id. 2000055.
[45] Dua, R., Z. Rashad, J. Spears, G. Dunn, and M. Maxwell. Applications of 3D-printed PEEK *via* fused filament fabrication: a systematic review. *Polymers*, Vol. 13, 2021, id. 4046.
[46] Oladapo, B. I., S. A. Zahedi, S. O. Ismail, and D. B. Olawade. Recent advances in biopolymeric composite materials: future sustainability of bone-implant. *Renewable and Sustainable Energy Reviews*, Vol. 150, 2021, id. 111505.
[47] Xu, W., S. Jambhulkar, Y. Zhu, D. Ravichandran, M. Kakarla, B. Vernon, et al. 3D printing for polymer/particle-based processing: a review. *Composites Part B: Engineering*, Vol. 223, 2021, id. 109102.
[48] Zhang, L., G. Yang, B. N. Johnson, and X. Jia. Three-dimensional (3D) printed scaffold and material selection for bone repair. *Acta Biomaterialia*, Vol. 84, 2019, pp. 16–33.
[49] Wu, W., J. Xin, B. Hu, R. Chen, D. Huang, Z. Huang, et al. Achieving injection molding interlayer strength *via* powder assisted hot isostatic pressing in material extrusion polyetheretherketone. *Additive Manufacturing*, Vol. 74, 2023, id. 103735.
[50] Lai, J., C. Wang, and M. Wang. 3D printing in biomedical engineering: processes, materials, and applications. *Applied Physics Reviews*, Vol. 8, 2021, id. 021322.
[51] Dua, R., Z. Rashad, J. Spears, G. Dunn, and M. Maxwell. Applications of 3D-printed PEEK *via* fused filament fabrication: a systematic review. *Polymers*, Vol. 13, 2021, id. 4046.
[52] Verma, S., N. Sharma, S. Kango, and S. Sharma. Developments of PEEK (polyetheretherketone) as a biomedical material: a focused review. *European Polymer Journal*, Vol. 147, 2021, id. 110295.
[53] Van De Werken, N., P. Koirala, J. Ghorbani, D. Doyle, and M. Tehrani. Investigating the hot isostatic pressing of an additively manufactured continuous carbon fiber reinforced PEEK composite. *Additive Manufacturing*, Vol. 37, 2021, id. 101634.
[54] Torstrick, F. B., A. S. P. Lin, D. Potter, D. L. Safranski, T. A. Sulchek, K. Gall, et al. Porous PEEK improves the bone-implant interface compared to plasma-sprayed titanium coating on PEEK. *Biomaterials*, Vol. 185, 2018, pp. 106–116.
[55] Sun, Y., S. Zhou, G. Qin, J. Guo, Q. Zhang, S. Li, et al. A chemical-induced crystallization strategy to fabricate poly(ether ether ketone) asymmetric membranes for organic solvent nanofiltration. *Journal of Membrane Science*, Vol. 620, 2021, id. 118899.
[56] Hughes, E. A. B. and L. M. Grover. Characterisation of a novel poly (ether ether ketone)/calcium sulphate composite for bone augmentation. *Biomaterial Research*, Vol. 21, 2017, id. 7.
[57] Corni, I., N. Neumann, S. Novak, K. König, P. Veronesi, Q. Chen, et al. Electrophoretic deposition of PEEK-nano alumina composite coatings on stainless steel. *Surface and Coatings Technology*, Vol. 203, 2009, pp. 1349–1359.
[58] Han, X., D. Yang, C. Yang, S. Spintzyk, L. Scheideler, P. Li, et al. Carbon fiber reinforced PEEK composites based on 3D-printing

technology for orthopedic and dental applications. *JCM*, Vol. 8, 2019, id. 240.
[59] Hamada, T., H. Fukasawa, S. Hasegawa, A. Miyashita, and Y. Maekawa. Graft-type polymer electrolyte membranes based on poly(ether ether ketone)/nanosilica hybrid films for fuel cell applications. *International Journal of Hydrogen Energy*, Vol. 41, 2016, pp. 18621–18630.
[60] Gao, S., S. Gao, B. Xu, and H. Yu. Effects of different pH-values on the nanomechanical surface properties of PEEK and CFR–PEEK compared to dental resin-based materials. *Materials*, Vol. 8, 2015, pp. 4751–4767.
[61] Kurtz, S. M. and J. N. Devine. PEEK biomaterials in trauma, orthopedic, and spinal implants. *Biomaterials*, Vol. 28, 2007, pp. 4845–4869.
[62] Sariyev, B., A. Abdikadyr, T. Baitikenov, Y. Anuarbekov, B. Golman, and C. Spitas. Thermal properties and mechanical behavior of hot pressed PEEK/graphite thin film laminate composites. *Scientific Reports*, Vol. 13, 2023, id. 12785.
[63] Hu, C., D. Ashok, D. R. Nisbet, and V. Gautam. Bioinspired surface modification of orthopedic implants for bone tissue engineering. *Biomaterials*, Vol. 219, 2019, id. 119366.
[64] Chen, B., J. Wang, and F. Yan. Comparative investigation on the tribological behaviors of CF/PEEK composites under sea water lubrication. *Tribology International*, Vol. 52, 2012, pp. 170–177.
[65] Andrew, J. J., H. Alhashmi, A. Schiffer, S. Kumar, and V. S. Deshpande. Energy absorption and self-sensing performance of 3D printed CF/PEEK cellular composites. *Materials and Design*, Vol. 208, 2021, id. 109863.
[66] Qin, W., Y. Li, J. Ma, Q. Liang, X. Cui, H. Jia, et al. Osseointegration and biosafety of graphene oxide wrapped porous CF/PEEK composites as implantable materials: the role of surface structure and chemistry. *Dental Materials*, Vol. 36, 2020, pp. 1289–1302.
[67] Yang, D., Y. Cao, Z. Zhang, Y. Yin, and D. Li. Effects of crystallinity control on mechanical properties of 3D-printed short-carbon-fiber-reinforced polyether ether ketone composites. *Polymer Testing*, Vol. 97, 2021, id. 107149.
[68] Hassan, E. A. M., D. Ge, S. Zhu, L. Yang, J. Zhou, and M. Yu. Enhancing CF/PEEK composites by CF decoration with polyimide and loosely-packed CNT arrays. *Composites Part A: Applied Science and Manufacturing*, Vol. 127, 2019, id. 105613.
[69] Chen, J., K. Wang, and Y. Zhao. Enhanced interfacial interactions of carbon fiber reinforced PEEK composites by regulating PEI and graphene oxide complex sizing at the interface. *Composites Science and Technology*, Vol. 154, 2018, pp. 175–186.
[70] Chen, Z., Y. Chen, J. Ding, and L. Yu. Blending strategy to modify PEEK-based orthopedic implants. *Composites Part B: Engineering*, Vol. 250, 2023, id. 110427.
[71] Su, Y., S. Zhang, X. Zhang, Z. Zhao, and D. Jing. Preparation and properties of carbon nanotubes/carbon fiber/poly (ether ether ketone) multiscale composites. *Composites Part A: Applied Science and Manufacturing*, Vol. 108, 2018, pp. 89–98.
[72] Ata, S., Y. Hayashi, T. B. Nguyen Thi, S. Tomonoh, S. Kawauchi, T. Yamada, et al. Improving thermal durability and mechanical properties of poly(ether ether ketone) with single-walled carbon nanotubes. *Polymer*, Vol. 176, 2019, pp. 60–65.
[73] Rong, C., G. Ma, S. Zhang, L. Song, Z. Chen, G. Wang, et al. Effect of carbon nanotubes on the mechanical properties and crystallization behavior of poly(ether ether ketone). *Composites Science and Technology*, Vol. 70, 2010, pp. 380–386.
[74] Theiler, G. and T. Gradt. Environmental effects on the sliding behaviour of PEEK composites. *Wear*, Vol. 368–369, 2016, pp. 278–286.
[75] Gong, F., K. Bui, D. V. Papavassiliou, and H. M. Duong. Thermal transport phenomena and limitations in heterogeneous polymer composites containing carbon nanotubes and inorganic nanoparticles. *Carbon*, Vol. 78, 2014, pp. 305–316.
[76] Mohammed, A. S. and M. I. Fareed. Improving the friction and wear of poly-ether-etherketone (PEEK) by using thin nano-composite coatings. *Wear*, Vol. 364–365, 2016, pp. 154–162.
[77] Feng, P., J. Jia, S. Peng, W. Yang, S. Bin, and C. Shuai. Graphene oxide-driven interfacial coupling in laser 3D printed PEEK/PVA scaffolds for bone regeneration. *Virtual and Physical Prototyping*, Vol. 15, 2020, pp. 211–226.
[78] He, M., X. Chen, Z. Guo, X. Qiu, Y. Yang, C. Su, et al. Super tough graphene oxide reinforced polyetheretherketone for potential hard tissue repair applications. *Composites Science and Technology*, Vol. 174, 2019, pp. 194–201.
[79] Awaja, F., M. Tripathi, T. Wong, T. O'Brien, and G. Speranza. The chemistry and topography of stabilized and functionalized graphene oxide coatings. *Plasma Processes and Polymers*, Vol. 15, 2018, id. 1800084.
[80] Shen, Y., L. Liang, S. Zhang, D. Huang, J. Zhang, S. Xu, et al. Organelle-targeting surface-enhanced Raman scattering (SERS) nanosensors for subcellular pH sensing. *Nanoscale*, Vol. 10, 2018, pp. 1622–1630.
[81] Ouyang, L., Y. Deng, L. Yang, X. Shi, T. Dong, Y. Tai, et al. Graphene-oxide-decorated microporous polyetheretherketone with superior antibacterial capability and in vitro osteogenesis for orthopedic implant. *Macromolecular Bioscience*, Vol. 18, 2018, id. 1800036.
[82] Wang, S., X. Zhao, Y. Hsu, Y. He, F. Wang, F. Yang, et al. Surface modification of titanium implants with Mg-containing coatings to promote osseointegration. *Acta Biomaterialia*, 2023, id. S1742706123004397.
[83] Kotsakis, G. A. and D. G. Olmedo. Peri-implantitis is not periodontitis: scientific discoveries shed light on microbiome-biomaterial interactions that may determine disease phenotype. *Periodontol 2000*, Vol. 86, 2021, pp. 231–240.
[84] Wu, S., J. Xu, L. Zou, S. Luo, R. Yao, B. Zheng, et al. Long-lasting renewable antibacterial porous polymeric coatings enable titanium biomaterials to prevent and treat peri-implant infection. *Nature Commununication*, Vol. 12, 2021, id. 3303.
[85] Baker, J. L., B. Bor, M. Agnello, W. Shi, and X. He. Ecology of the oral microbiome: beyond bacteria. *Trends in Microbiology*, Vol. 25, 2017, pp. 362–374.
[86] Gao, L., T. Xu, G. Huang, S. Jiang, Y. Gu, and F. Chen. Oral microbiomes: more and more importance in oral cavity and whole body. *Protein Cell*, Vol. 9, 2018, pp. 488–500.
[87] Gulati, K., D. Chopra, N. A. Kocak-Oztug, and E. Verron. Fit and forget: the future of dental implant therapy *via* nanotechnology. *Advanced Drug Delivery Reviews*, Vol. 199, 2023, id. 114900.
[88] Mazmanian, S. K., C. H. Liu, A. O. Tzianabos, and D. L. Kasper. An immunomodulatory molecule of symbiotic bacteria directs maturation of the host immune system. *Cell*, Vol. 122, 2005, pp. 107–118.
[89] Huang, Y., Y. Liu, S. Shah, D. Kim, A. Simon-Soro, T. Ito, et al. Precision targeting of bacterial pathogen *via* bi-functional nanozyme activated by biofilm microenvironment. *Biomaterials*, Vol. 268, 2021, id. 120581.

[90] Le, N.-H., V. Pinedo, J. Lopez, F. Cava, and M. F. Feldman. Killing of gram-negative and gram-positive bacteria by a bifunctional cell wall-targeting T6SS effector. *Proceedings of the National Academy of Sciences U S A*, Vol. 118, 2021, id. e2106555118.
[91] Shaikh, S., N. Nazam, S. M. D. Rizvi, K. Ahmad, M. H. Baig, E. J. Lee, et al. Mechanistic insights into the antimicrobial actions of metallic nanoparticles and their implications for multidrug resistance. *IJMS*, Vol. 20, 2019, id. 2468.
[92] Lee, S. and B.-H. Jun. Silver nanoparticles: synthesis and application for nanomedicine. *IJMS*, Vol. 20, 2019, id. 865.
[93] Qin, Z., Y. Zheng, Y. Wang, T. Du, C. Li, X. Wang, et al. Versatile roles of silver in Ag-based nanoalloys for antibacterial applications. *Coordination Chemistry Reviews*, Vol. 449, 2021, id. 214218.
[94] Kędziora, A., M. Speruda, E. Krzyżewska, J. Rybka, A. Łukowiak, and G. Bugla-Płoskońska. Similarities and differences between silver ions and silver in nanoforms as antibacterial agents. *IJMS*, Vol. 19, 2018, id. 444.
[95] Roy, A., O. Bulut, S. Some, A. K. Mandal, and M. D. Yilmaz. Green synthesis of silver nanoparticles: biomolecule-nanoparticle organizations targeting antimicrobial activity. *RSC Advances*, Vol. 9, 2019, pp. 2673–2702.
[96] Liu, X., K. Gan, H. Liu, X. Song, T. Chen, and C. Liu. Antibacterial properties of nano-silver coated PEEK prepared through magnetron sputtering. *Dental Materials*, Vol. 33, 2017, pp. e348–e360.
[97] Deng, L., Y. Deng, and K. Xie. AgNPs-decorated 3D printed PEEK implant for infection control and bone repair. *Colloids and Surfaces B: Biointerfaces*, Vol. 160, 2017, pp. 483–492.
[98] Girard, J., N. Joset, A. Crochet, M. Tan, A. Holzheu, P. Brunetto, et al. Synthesis of new polyether ether ketone derivatives with silver binding site and coordination compounds of their monomers with different silver salts. *Polymers*, Vol. 8, 2016, id. 208.
[99] Yu, Y., Y. Sun, X. Zhou, Y. Mao, Y. Liu, L. Ye, et al. Ag and peptide Co-decorate polyetheretherketone to enhance antibacterial property and osteogenic differentiation. *Colloids and Surfaces B: Biointerfaces*, Vol. 198, 2021, id. 111492.
[100] Nawaz, Q., S. Fastner, M. A. U. Rehman, S. Ferraris, S. Perero, G. G. Di Confiengo, et al. Multifunctional stratified composite coatings by electrophoretic deposition and RF Co-sputtering for orthopaedic implants. *Journal of Materials Science*, Vol. 56, 2021, pp. 7920–7935.
[101] Nawaz, A., S. Bano, M. Yasir, A. Wadood, and M. A. Ur Rehman. Ag and Mn-doped mesoporous bioactive glass nanoparticles incorporated into the chitosan/gelatin coatings deposited on PEEK/bioactive glass layers for favorable osteogenic differentiation and antibacterial activity. *Materials Advances*, Vol. 1, 2020, pp. 1273–1284.
[102] Ramstedt, M., B. Ekstrand-Hammarström, A. V. Shchukarev, A. Bucht, L. Österlund, M. Welch, et al. Bacterial and mammalian cell response to poly(3-sulfopropyl methacrylate) brushes loaded with silver halide salts. *Biomaterials*, Vol. 30, 2009, pp. 1524–1531.
[103] Das, K., S. Bose, A. Bandyopadhyay, B. Karandikar, and B. L. Gibbins. Surface coatings for improvement of bone cell materials and antimicrobial activities of Ti implants. *Journal of Biomedical Materials Research*, Vol. 87B, 2008, pp. 455–460.
[104] Ariöz, C. and P. Wittung-Stafshede. Folding of copper proteins: role of the metal? *Quarterly Reviews of Biophysics*, Vol. 51, 2018, id. e4.
[105] Yan, J., D. Xia, W. Zhou, Y. Li, P. Xiong, Q. Li, et al. pH-responsive silk fibroin-based CuO/Ag micro/nano coating endows polyetheretherketone with synergistic antibacterial ability, osteogenesis, and angiogenesis. *Acta Biomaterialia*, Vol. 115, 2020, pp. 220–234.
[106] Wang, L., R. Peng, X. Liu, C. Heng, Y. Miao, W. Wang, et al. Nitrite-enhanced copper-based fenton reactions for biofilm removal. *Chemical Communications*, Vol. 57, 2021, pp. 5514–5517.
[107] Fan, X., L. Yahia, and E. Sacher. Antimicrobial properties of the Ag, Cu nanoparticle system. *Biology*, Vol. 10, 2021, id. 137.
[108] Andrei, A., Y. Öztürk, B. Khalfaoui-Hassani, J. Rauch, D. Marckmann, P.-I. Trasnea, et al. Cu homeostasis in bacteria: the ins and outs. *Membranes*, Vol. 10, 2020, id. 242.
[109] Vincent, M., R. E. Duval, P. Hartemann, and M. Engels-Deutsch. Contact killing and antimicrobial properties of copper. *Journal of Applied Microbiology*, Vol. 124, 2018, pp. 1032–1046.
[110] Wu, Y., W. Wu, W. Zhao, and X. Lan. Revealing the antibacterial mechanism of copper surfaces with controllable microstructures. *Surface and Coatings Technology*, Vol. 395, 2020, id. 125911.
[111] Liu, W., J. Li, M. Cheng, Q. Wang, Y. Qian, K. W. K. Yeung, et al. A surface-engineered polyetheretherketone biomaterial implant with direct and immunoregulatory antibacterial activity against methicillin-resistant *staphylococcus aureus*. *Biomaterials*, Vol. 208, 2019, pp. 8–20.
[112] Yan, J., D. Xia, P. Xiong, Y. Li, W. Zhou, Q. Li, et al. Polyetheretherketone with citrate potentiated influx of copper boosts osteogenesis, angiogenesis, and bacteria-triggered antibacterial abilities. *Journal of Materials Science and Technology*, Vol. 71, 2021, pp. 31–43.
[113] Wang, L., H. He, X. Yang, Y. Zhang, S. Xiong, C. Wang, et al. Bimetallic ions regulated PEEK of bone implantation for antibacterial and osteogenic activities. *Materials Today Advances*, Vol. 12, 2021, id. 100162.
[114] Ye, Q., W. Chen, H. Huang, Y. Tang, W. Wang, F. Meng, et al. Iron and zinc ions, potent weapons against multidrug-resistant bacteria. *Applied Microbiology and Biotechnology*, Vol. 104, 2020, pp. 5213–5227.
[115] Arakha, M., S. Pal, D. Samantarrai, T. K. Panigrahi, B. C. Mallick, K. Pramanik, et al. Antimicrobial activity of iron oxide nanoparticle upon modulation of nanoparticle-bacteria interface. *Scientific Reports*, Vol. 5, 2015, id. 14813.
[116] Belenky, P., J. D. Ye, C. B. M. Porter, N. R. Cohen, M. A. Lobritz, T. Ferrante, et al. Bactericidal antibiotics induce toxic metabolic perturbations that lead to cellular damage. *Cell Reports*, Vol. 13, 2015, pp. 968–980.
[117] Zhang, J., X. Gao, D. Ma, S. He, B. Du, W. Yang, et al. Copper ferrite heterojunction coatings empower polyetheretherketone implant with multi-modal bactericidal functions and boosted osteogenicity through synergistic photo/fenton-therapy. *Chemical Engineering Journal*, Vol. 422, 2021, id. 130094.
[118] Zhang, J., P. Liu, Y. Ren, Y. Du, C. Geng, J. Ma, et al. Treatment of shale gas produced water by magnetic $CuFe_2O_4$/TNTs hybrid heterogeneous catalyzed ozone: efficiency and mechanisms. *Journal of Hazardous Materials*, Vol. 423, 2022, id. 127124.
[119] Sirelkhatim, A., S. Mahmud, A. Seeni, N. H. M. Kaus, L. C. Ann, S. K. M. Bakhori, et al. Review on zinc oxide nanoparticles: antibacterial activity and toxicity mechanism. *Nano-Micro Letters*, Vol. 7, 2015, pp. 219–242.
[120] Hadley, K. B., S. M. Newman, and J. R. Hunt. Dietary zinc reduces osteoclast resorption activities and increases markers of osteoblast differentiation, matrix maturation, and mineralization in the long bones of growing rats. *The Journal of Nutritional Biochemistry*, Vol. 21, 2010, pp. 297–303.

[121] Jafarirad, S., M. Mehrabi, B. Divband, and M. Kosari-Nasab. Biofabrication of zinc oxide nanoparticles using fruit extract of rosa canina and their toxic potential against bacteria: a mechanistic approach. *Materials Science and Engineering: C*, Vol. 59, 2016, pp. 296–302.

[122] Nairn, B. L., Z. R. Lonergan, J. Wang, J. J. Braymer, Y. Zhang, M. W. Calcutt, et al. The response of acinetobacter baumannii to zinc starvation. *Cell Host and Microbe*, Vol. 19, 2016, pp. 826–836.

[123] Jin, G., H. Qin, H. Cao, S. Qian, Y. Zhao, X. Peng, et al. Synergistic effects of dual Zn/Ag ion implantation in osteogenic activity and antibacterial ability of titanium. *Biomaterials*, Vol. 35, 2014, pp. 7699–7713.

[124] Yu, F., X. Fang, H. Jia, M. Liu, X. Shi, C. Xue, et al. Zn or O? an atomic level comparison on antibacterial activities of zinc oxides. *Chemistry—A European Journal*, Vol. 22, 2016, pp. 8053–8058.

[125] Augustine, R., H. N. Malik, D. K. Singhal, A. Mukherjee, D. Malakar, N. Kalarikkal, et al. Electrospun polycaprolactone/ZnO nanocomposite membranes as biomaterials with antibacterial and cell adhesion properties. *Journal of Polymer Research*, Vol. 21, 2014, id. 347.

[126] Yu, X., M. Ibrahim, Z. Liu, H. Yang, L. Tan, and K. Yang. Biofunctional Mg coating on PEEK for improving bioactivity. *Bioactive Materials*, Vol. 3, 2018, pp. 139–143.

[127] Li, C.-H., C.-C. Shen, Y.-W. Cheng, S.-H. Huang, C.-C. Wu, C.-C. Kao, et al. Organ biodistribution, clearance, and genotoxicity of orally administered zinc oxide nanoparticles in mice. *Nanotoxicology*, Vol. 6, 2012, pp. 746–756.

[128] Sayes, C. M., K. L. Reed, and D. B. Warheit. Assessing toxicity of fine and nanoparticles: comparing in vitro measurements to *in vivo* pulmonary toxicity profiles. *Toxicological Sciences*, Vol. 97, 2007, pp. 163–180.

[129] Yu, Y., Y. Sun, X. Zhou, Y. Mao, Y. Liu, L. Ye, et al. Ag and peptide Co-decorate polyetheretherketone to enhance antibacterial property and osteogenic differentiation. *Colloids and Surfaces B: Biointerfaces*, Vol. 198, 2021, id. 111492.

[130] Fan, X., L. Yahia, and E. Sacher. Antimicrobial properties of the Ag, Cu nanoparticle system. *Biology*, Vol. 10, 2021, id. 137.

[131] Andrei, A., Y. Öztürk, B. Khalfaoui-Hassani, J. Rauch, D. Marckmann, P.-I. Trasnea, et al. Cu homeostasis in bacteria: the ins and outs. *Membranes*, Vol. 10, 2020, id. 242.

[132] Wang, L., R. Peng, X. Liu, C. Heng, Y. Miao, W. Wang, et al. Nitrite-enhanced copper-based fenton reactions for biofilm removal. *Chemical Communications*, Vol. 57, 2021, pp. 5514–5517.

[133] Yan, J., D. Xia, W. Zhou, Y. Li, P. Xiong, Q. Li, et al. pH-responsive silk fibroin-based CuO/Ag micro/nano coating endows polyetheretherketone with synergistic antibacterial ability, osteogenesis, and angiogenesis. *Acta Biomaterialia*, Vol. 115, 2020, pp. 220–234.

[134] Nawaz, Q., S. Fastner, M. A. U. Rehman, S. Ferraris, S. Perero, G. G. Di Confiengo, et al. Multifunctional stratified composite coatings by electrophoretic deposition and RF Co-sputtering for orthopaedic implants. *Journal of Materials Science*, Vol. 56, 2021, pp. 7920–7935.

[135] Nawaz, A., S. Bano, M. Yasir, A. Wadood, and M. A. Ur Rehman. Ag and Mn-doped mesoporous bioactive glass nanoparticles incorporated into the chitosan/gelatin coatings deposited on PEEK/bioactive glass layers for favorable osteogenic differentiation and antibacterial activity. *Materials Advances*, Vol. 1, 2020, pp. 1273–1284.

[136] Zhang, J., X. Gao, D. Ma, S. He, B. Du, W. Yang, et al. Copper ferrite heterojunction coatings empower polyetheretherketone implant with multi-modal bactericidal functions and boosted osteogenicity through synergistic photo/fenton-therapy. *Chemical Engineering Journal*, Vol. 422, 2021, id. 130094.

[137] Wang, L., H. He, X. Yang, Y. Zhang, S. Xiong, C. Wang, et al. Bimetallic ions regulated PEEK of bone implantation for antibacterial and osteogenic activities. *Materials Today Advances*, Vol. 12, 2021, id. 100162.

[138] Díez-Pascual, A. M., C. Xu, and R. Luque. Development and characterization of novel poly(ether ether ketone)/ZnO bionanocomposites. *Journal of Materials Chemistry B*, Vol. 2, 2014, id. 3065.

[139] Tao, T., I.-T. Bae, K. B. Woodruff, K. Sauer, and J. Cho. Hydrothermally-grown nanostructured anatase TiO_2 coatings tailored for photocatalytic and antibacterial properties. *Ceramics International*, Vol. 45, 2019, pp. 23216–23224.

[140] Xian, P., Y. Chen, S. Gao, J. Qian, W. Zhang, A. Udduttula, et al. Polydopamine (PDA) mediated nanogranular-structured titanium dioxide (TiO_2) coating on polyetheretherketone (PEEK) for oral and maxillofacial implants application. *Surface and Coatings Technology*, Vol. 401, 2020, id. 126282.

[141] Bock, R. M., E. N. Jones, D. A. Ray, B. Sonny Bal, G. Pezzotti, and B. J. McEntire. Bacteriostatic behavior of surface modulated silicon nitride in comparison to polyetheretherketone and titanium: bacteriostatic behavior of surface modulated silicon nitride. *Journal of Biomedical Materials Research*, Vol. 105, 2017, pp. 1521–1534.

[142] Bal, S., D. Gorth, S. Puckett, T. J. Webster, Rahaman, and B. Ercan. Decreased bacteria activity on Si3N4 surfaces compared with PEEK or titanium. *IJN*, 2012, id. 4829.

[143] Pezzotti, G., E. Marin, T. Adachi, F. Lerussi, A. Rondinella, F. Boschetto, et al. Incorporating Si_3N_4 into PEEK to produce antibacterial, osteocondutive, and radiolucent spinal implants. *Macromolecular Bioscience*, Vol. 18, 2018, id. 1800033.

[144] Xian, P., Y. Chen, S. Gao, J. Qian, W. Zhang, A. Udduttula, et al. Polydopamine (PDA) mediated nanogranular-structured titanium dioxide (TiO_2) coating on polyetheretherketone (PEEK) for oral and maxillofacial implants application. *Surface and Coatings Technology*, Vol. 401, 2020, id. 126282.

[145] Webster, T. J., A. A. Patel, M. N. Rahaman, and B. Sonny Bal. Anti-infective and osteointegration properties of silicon nitride, poly (ether ether ketone), and titanium implants. *Acta Biomaterialia*, Vol. 8, 2012, pp. 4447–4454.

[146] Bock, R. M., E. N. Jones, D. A. Ray, B. Sonny Bal, G. Pezzotti, and B. J. McEntire. Bacteriostatic behavior of surface modulated silicon nitride in comparison to polyetheretherketone and titanium. *Journal of Biomedical Materials Research*, Vol. 105, 2017, pp. 1521–1534.

[147] Gorth, D. J., S. Puckett, B. Ercan, T. J. Webster, M. Rahaman, and B. S. Bal. Decreased bacteria activity on Si_3N_4 surfaces compared with PEEK or titanium. *IJN*, 2012, id. 4829.

[148] Pezzotti, G., E. Marin, T. Adachi, F. Lerussi, A. Rondinella, F. Boschetto, et al. Incorporating Si_3N_4 into PEEK to produce antibacterial, osteocondutive, and radiolucent spinal implants. *Macromolecular Bioscience*, Vol. 18, 2018, id. 1800033.

[149] Chen, T., Q. Chen, H. Fu, D. Wang, Y. Gao, M. Zhang, et al. Construction and performance evaluation of a sustained release implant material polyetheretherketone with antibacterial properties. *Materials Science and Engineering: C*, Vol. 126, 2021, id. 112109.

[150] Zou, F., F. Lv, X. Ma, X. Xia, L. Cai, S. Mei, et al. Dual drugs release from nanoporously bioactive coating on polyetheretherketone

for enhancement of antibacterial activity, rBMSCs responses and osseointegration. *Materials and Design*, Vol. 188, 2020, id. 108433.
[151] Gao, C., Z. Wang, Z. Jiao, Z. Wu, M. Guo, Y. Wang, et al. Enhancing antibacterial capability and osseointegration of polyetheretherketone (PEEK) implants by dual-functional surface modification. *Materials and Design*, Vol. 205, 2021, id. 109733.
[152] Xue, Z., Z. Wang, A. Sun, J. Huang, W. Wu, M. Chen, et al. Rapid construction of polyetheretherketone (PEEK) biological implants incorporated with brushite ($CaHPO_4{\cdot}2H_2O$) and antibiotics for anti-infection and enhanced osseointegration. *Materials Science and Engineering: C*, Vol. 111, 2020, id. 110782.
[153] Xu, X., Y. Li, L. Wang, Y. Li, J. Pan, X. Fu, et al. Triple-functional polyetheretherketone surface with enhanced bacteriostasis and anti-inflammatory and osseointegrative properties for implant application. *Biomaterials*, Vol. 212, 2019, pp. 98–114.
[154] AbouAitah, K., M. Bil, E. Pietrzykowska, U. Szałaj, D. Fudala, B. Woźniak, et al. Drug-releasing antibacterial coating made from nano-hydroxyapatite using the sonocoating method. *Nanomaterials*, Vol. 11, 2021, id. 1690.
[155] Sang, S., C. Yang, H. Chai, X. Yuan, W. Liu, and X. Zhang. The sulfonated polyetheretherketone with 3D structure modified by two bio-inspired methods shows osteogenic and antibacterial functions. *Chemical Engineering Journal*, Vol. 420, 2021, id. 130059.
[156] Yuan, X., L. Ouyang, Y. Luo, Z. Sun, C. Yang, J. Wang, et al. Multifunctional sulfonated polyetheretherketone coating with beta-defensin-14 for yielding durable and broad-spectrum antibacterial activity and osseointegration. *Acta Biomaterialia*, Vol. 86, 2019, pp. 323–337.
[157] Li, M., J. Bai, H. Tao, L. Hao, W. Yin, X. Ren, et al. Rational integration of defense and repair synergy on PEEK osteoimplants *via* biomimetic peptide clicking strategy. *Bioactive Materials*, Vol. 8, 2022, pp. 309–324.
[158] He, X., Y. Deng, Y. Yu, H. Lyu, and L. Liao. Drug-loaded/grafted peptide-modified porous PEEK to promote bone tissue repair and eliminate bacteria. *Colloids and Surfaces B: Biointerfaces*, Vol. 181, 2019, pp. 767–777.
[159] Zou, F., F. Lv, X. Ma, X. Xia, L. Cai, S. Mei, et al. Dual drugs release from nanoporously bioactive coating on polyetheretherketone for enhancement of antibacterial activity, rBMSCs responses and osseointegration. *Materials and Design*, Vol. 188, 2020, id. 108433.
[160] Ekambaram, R., V. Paraman, L. Raja, M. K. Suresh, and S. Dharmalingam. Design and development of electrospun SPEEK incorporated with aminated zirconia and curcumin nanofibers for periodontal regeneration. *Journal of the Mechanical Behavior of Biomedical Materials*, Vol. 123, 2021, id. 104796.
[161] Sang, S., S. Wang, C. Yang, Z. Geng, and X. Zhang. Sponge-inspired sulfonated polyetheretherketone loaded with polydopamine-protected osthole nanoparticles and berberine enhances osteogenic activity and prevents implant-related infections. *Chemical Engineering Journal*, Vol. 437, 2022, id. 135255.
[162] Nawaz, A. and M. A. Ur Rehman. Chitosan/gelatin-based bioactive and antibacterial coatings deposited *via* electrophoretic deposition. *Journal of Applied Polymer Science*, Vol. 138, 2021, id. 50220.
[163] Ter Boo, G.-J. A., D. W. Grijpma, T. F. Moriarty, R. G. Richards, and D. Eglin. Antimicrobial delivery systems for local infection prophylaxis in orthopedic- and trauma surgery. *Biomaterials*, Vol. 52, 2015, pp. 113–125.
[164] Bellows, C. F., K. T. Mills, T. N. Kelly, and G. Gagliardi. Combination of oral non-absorbable and intravenous antibiotics versus intravenous antibiotics alone in the prevention of surgical site infections after colorectal surgery: a meta-analysis of randomized controlled trials. *Techniques in coloproctology*, Vol. 15, 2011, pp. 385–395.
[165] Delaney, L. J., D. MacDonald, J. Leung, K. Fitzgerald, A. M. Sevit, J. R. Eisenbrey, et al. Ultrasound-triggered antibiotic release from PEEK clips to prevent spinal fusion infection: initial evaluations. *Acta Biomaterialia*, Vol. 93, 2019, pp. 12–24.
[166] Delaney, L. J., C. Basgul, D. W. MacDonald, K. Fitzgerald, N. J. Hickok, S. M. Kurtz, et al. Acoustic parameters for optimal ultrasound-triggered release from novel spinal hardware devices. *Ultrasound in Medicine and Biology*, Vol. 46, 2020, pp. 350–358.
[167] Chen, T., Q. Chen, H. Fu, D. Wang, Y. Gao, M. Zhang, et al. Construction and performance evaluation of a sustained release implant material polyetheretherketone with antibacterial properties. *Materials Science and Engineering: C*, Vol. 126, 2021, id. 112109.
[168] Gao, C., Z. Wang, Z. Jiao, Z. Wu, M. Guo, Y. Wang, et al. Enhancing antibacterial capability and osseointegration of polyetheretherketone (PEEK) implants by dual-functional surface modification. *Materials and Design*, Vol. 205, 2021, id. 109733.
[169] Xue, Z., Z. Wang, A. Sun, J. Huang, W. Wu, M. Chen, et al. Rapid construction of polyetheretherketone (PEEK) biological implants incorporated with brushite ($CaHPO_4{\cdot}2H_2O$) and antibiotics for anti-infection and enhanced osseointegration. *Materials Science and Engineering: C*, Vol. 111, 2020, id. 110782.
[170] Xu, X., Y. Li, L. Wang, Y. Li, J. Pan, X. Fu, et al. Triple-functional polyetheretherketone surface with enhanced bacteriostasis and anti-inflammatory and osseointegrative properties for implant application. *Biomaterials*, Vol. 212, 2019, pp. 98–114.
[171] Asadi, A., M. Abdi, E. Kouhsari, P. Panahi, M. Sholeh, N. Sadeghifard, et al. Minocycline, focus on mechanisms of resistance, antibacterial activity, and clinical effectiveness: back to the future. *Journal of Global Antimicrobial Resistance*, Vol. 22, 2020, pp. 161–174.
[172] AbouAitah, K., M. Bil, E. Pietrzykowska, U. Szałaj, D. Fudala, B. Woźniak, et al. Drug-releasing antibacterial coating made from nano-hydroxyapatite using the sonocoating method. *Nanomaterials*, Vol. 11, 2021, id. 1690.
[173] Sang, S., C. Yang, H. Chai, X. Yuan, W. Liu, and X. Zhang. The sulfonated polyetheretherketone with 3D structure modified by two bio-inspired methods shows osteogenic and antibacterial functions. *Chemical Engineering Journal*, Vol. 420, 2021, id. 130059.
[174] Sang, S., G. Guo, J. Yu, and X. Zhang. Antibacterial application of gentamicin–silk protein coating with smart release function on titanium, polyethylene, and Al_2O_3 materials. *Materials Science and Engineering: C*, Vol. 124, 2021, id. 112069.
[175] Santos, V. F., A. C. J. Araújo, P. R. Freitas, A. L. P. Silva, A. L. E. Santos, B. A. Matias Da Rocha, et al. Enhanced antibacterial activity of the gentamicin against multidrug-resistant strains when complexed with canavalia ensiformis lectin. *Microbial Pathogenesis*, Vol. 152, 2021, id. 104639.
[176] Mookherjee, N., M. A. Anderson, H. P. Haagsman, and D. J. Davidson. Antimicrobial host defence peptides: functions and clinical potential. *Nature Reviews Drug Discovery*, Vol. 19, 2020, pp. 311–332.
[177] Wei, D. and X. Zhang. Biosynthesis, bioactivity, biotoxicity and applications of antimicrobial peptides for human health. *Biosafety and Health*, Vol. 4, 2022, pp. 118–134.
[178] Li, M., J. Bai, H. Tao, L. Hao, W. Yin, X. Ren, et al. Rational integration of defense and repair synergy on PEEK osteoimplants *via*

biomimetic peptide clicking strategy. *Bioactive Materials*, Vol. 8, 2022, pp. 309–324.
[179] Chen, J., X. Shi, Y. Zhu, Y. Chen, M. Gao, H. Gao, et al. On-demand storage and release of antimicrobial peptides using pandora's box-like nanotubes gated with a bacterial infection-responsive polymer. *Theranostics*, Vol. 10, 2020, pp. 109–122.
[180] Yuan, X., L. Ouyang, Y. Luo, Z. Sun, C. Yang, J. Wang, et al. Multifunctional sulfonated polyetheretherketone coating with beta-defensin-14 for yielding durable and broad-spectrum antibacterial activity and osseointegration. *Acta Biomaterialia*, Vol. 86, 2019, pp. 323–337.
[181] Yue, H., L. Yuan, W. Zhang, S. Zhang, W. Wei, and G. Ma. Macrophage responses to the physical burden of cell-sized particles. *Journal of Materials Chemistry B*, Vol. 6, 2018, pp. 393–400.
[182] He, X., Y. Deng, Y. Yu, H. Lyu, and L. Liao. Drug-loaded/grafted peptide-modified porous PEEK to promote bone tissue repair and eliminate bacteria. *Colloids and Surfaces B: Biointerfaces*, Vol. 181, 2019, pp. 767–777.
[183] Boerjan, W., J. Ralph, and M. Baucher. Lignin biosynthesis. *Annual Review of Plant Biology*, Vol. 54, 2003, pp. 519–546.
[184] He, X., Y. Deng, Y. Yu, H. Lyu, and L. Liao. Drug-loaded/grafted peptide-modified porous PEEK to promote bone tissue repair and eliminate bacteria. *Colloids and Surfaces B: Biointerfaces*, Vol. 181, 2019, pp. 767–777.
[185] Zou, F., F. Lv, X. Ma, X. Xia, L. Cai, S. Mei, et al. Dual drugs release from nanoporously bioactive coating on polyetheretherketone for enhancement of antibacterial activity, rBMSCs responses and osseointegration. *Materials and Design*, Vol. 188, 2020, id. 108433.
[186] Ekambaram, R., V. Paraman, L. Raja, M. K. Suresh, and S. Dharmalingam. Design and development of electrospun SPEEK incorporated with aminated zirconia and curcumin nanofibers for periodontal regeneration. *Journal of the Mechanical Behavior of Biomedical Materials*, Vol. 123, 2021, id. 104796.
[187] Sang, S., S. Wang, C. Yang, Z. Geng, and X. Zhang. Sponge-inspired sulfonated polyetheretherketone loaded with polydopamine-protected osthole nanoparticles and berberine enhances osteogenic activity and prevents implant-related infections. *Chemical Engineering Journal*, Vol. 437, 2022, id. 135255.
[188] Khoury, J., E. R. Edelman, C. Talmo, and T. J. Webster. Accelerated neutral atom beam (ANAB) modified polyethylene for decreased wear and reduced bacteria colonization: an in vitro study. *Nanomedicine: Nanotechnology, Biology and Medicine*, Vol. 42, 2022, id. 102540.
[189] Ajami, S., M. J. Coathup, J. Khoury, and G. W. Blunn. Augmenting the bioactivity of polyetheretherketone using a novel accelerated neutral atom beam technique. *Journal of Biomedical Materials Research*, Vol. 105, 2017, pp. 1438–1446.
[190] Durham, J. W. and A. Rabiei. Deposition, heat treatment and characterization of two layer bioactive coatings on cylindrical PEEK. *Surface and Coatings Technology*, Vol. 301, 2016, pp. 106–113.
[191] Durham, J. W., M. J. Allen, and A. Rabiei. Preparation, characterization and *in vitro* response of bioactive coatings on polyether ether ketone: response of bioactive coatings on polyether ether ketone. *Journal of Biomedical Materials Research*, Vol. 105, 2017, pp. 560–567.
[192] Štefaníková, R., T. Kretková, A. Kuzminova, J. Hanuš, M. Vaidulych, O. Kylián, et al. Influence of atmospheric pressure dielectric barrier discharge on wettability and drying of poly(ether-ether-ketone) foils. *Polymer Degradation and Stability*, Vol. 150, 2018, pp. 114–121.
[193] Liu, C., J. Bai, Y. Wang, L. Chen, D. Wang, S. Ni, et al. The effects of three cold plasma treatments on the osteogenic activity and antibacterial property of PEEK. *Dental Materials*, Vol. 37, 2021, pp. 81–93.
[194] Fu, Q., M. Gabriel, F. Schmidt, W.-D. Müller, and A. D. Schwitalla. The impact of different low-pressure plasma types on the physical, chemical and biological surface properties of PEEK. *Dental Materials*, Vol. 37, 2021, pp. e15–e22.
[195] Wang, S., Y. Deng, L. Yang, X. Shi, W. Yang, and Z.-G. Chen. Enhanced antibacterial property and osteo-differentiation activity on plasma treated porous polyetheretherketone with hierarchical micro/nano-topography. *Journal of Biomaterials Science, Polymer Edition*, Vol. 29, 2018, pp. 520–542.
[196] Yu, W., H. Zhang, A. Lan, S. Yang, J. Zhang, H. Wang, et al. Enhanced bioactivity and osteogenic property of carbon fiber reinforced polyetheretherketone composites modified with amino groups. *Colloids and Surfaces B: Biointerfaces*, Vol. 193, 2020, id. 111098.
[197] Lu, T., S. Qian, F. Meng, C. Ning, and X. Liu. Enhanced osteogenic activity of poly ether ether ketone using calcium plasma immersion ion implantation. *Colloids and Surfaces B: Biointerfaces*, Vol. 142, 2016, pp. 192–198.
[198] Yue, H., L. Yuan, W. Zhang, S. Zhang, W. Wei, and G. Ma. Macrophage responses to the physical burden of cell-sized particles. *Journal of Materials Chemistry B*, Vol. 6, 2018, pp. 393–400.
[199] Johansson, P., R. Jimbo, P. Kjellin, B. Chrcanovic, A. Wennerberg, and F. Currie. Biomechanical evaluation and surface characterization of a nano-modified surface on PEEK implants: A study in the Rabbit Tibia. *International Journal of nanomedicine*, Vol. 9, 2014, pp. 3903–3911.
[200] Lu, T., J. Li, S. Qian, H. Cao, C. Ning, and X. Liu. Enhanced osteogenic and selective antibacterial activities on micro-/nano-structured carbon fiber reinforced polyetheretherketone. *Journal of Materials Chemistry B*, Vol. 4, 2016, pp. 2944–2953.
[201] Sargin, F., G. Erdogan, K. Kanbur, and A. Turk. Investigation of in vitro behavior of plasma sprayed Ti, TiO_2 and HA coatings on PEEK. *Surface and Coatings Technology*, Vol. 411, 2021, id. 126965.
[202] Deng, F., X. Wu, X. Liu, and S. Wei. Nano-TiO_2/PEEK bioactive composite as a bone substitute material: in vitro and *in vivo* studies. *IJN*, 2012, id. 1215.
[203] Lu, W.-J., V. Srimaneepong, C.-S. Chen, C.-H. Huang, H.-C. Lin, C.-F. Liu, et al. Influence of aging on the fracture characteristics of polyetheretherketone dental crowns: a preliminary study. *Polymers*, Vol. 14, 2022, id. 4123.
[204] Shimizu, T., S. Fujibayashi, S. Yamaguchi, B. Otsuki, Y. Okuzu, T. Matsushita, et al. In vivo experimental study of anterior cervical fusion using bioactive polyetheretherketone in a canine model. *PLoS ONE*, Vol. 12, 2017, id. e0184495.
[205] Wu, J., L. Li, C. Fu, F. Yang, Z. Jiao, X. Shi, et al. Micro-porous polyetheretherketone implants decorated with BMP-2 *via* phosphorylated gelatin coating for enhancing cell adhesion and osteogenic differentiation. *Colloids and Surfaces B: Biointerfaces*, Vol. 169, 2018, pp. 233–241.
[206] Zhang, R., J.-I. Jo, R. Kanda, A. Nishiura, Y. Hashimoto, and N. Matsumoto. Bioactive polyetheretherketone with gelatin hydrogel leads to sustained release of bone morphogenetic protein-2 and promotes osteogenic differentiation. *IJMS*, Vol. 24, 2023, id. 12741.
[207] Zheng, Y., H. Zhou, M. Li, J. Fu, J. Dong, Y. Liu, et al. Polyetheretherketone surface engineered with a degradable

hybrid coating for accelerating osteogenesis. *Materials Letters*, Vol. 331, 2023, id. 133515.
[208] Zheng, Y., A. Gao, J. Bai, Q. Liao, Y. Wu, W. Zhang, et al. A programmed surface on polyetheretherketone for sequentially dictating osteoimmunomodulation and bone regeneration to achieve ameliorative osseointegration under osteoporotic conditions. *Bioactive Materials*, Vol. 14, 2022, pp. 364–376.
[209] Zheng, J., H. Zhao, Z. Ouyang, X. Zhou, J. Kang, C. Yang, et al. Additively-manufactured PEEK/HA porous scaffolds with excellent osteogenesis for bone tissue repairing. *Composites Part B: Engineering*, Vol. 232, 2022, id. 109508.
[210] Yakufu, M., Z. Wang, J. Liu, and P. Zhang. Bionic manufacturing strategy of hydroxyapatite-coated polyether ether ketone scaffolds for promoting mineralization and osseointegration. *Materials and Design*, Vol. 223, 2022, id. 111193.
[211] Ma, R., Z. Yu, S. Tang, Y. Pan, J. Wei, and T. Tang. Osseointegration of nanohydroxyapatite- or nano-calcium silicate-incorporated polyetheretherketone bioactive composites in vivo. *IJN*, Vol. 11, 2016, pp. 6023–6033.
[212] Zhao, Y., H. M. Wong, W. Wang, P. Li, Z. Xu, E. Y. W. Chong, et al. Cytocompatibility, osseointegration, and bioactivity of three-dimensional porous and nanostructured network on polyetheretherketone. *Biomaterials*, Vol. 34, 2013, pp. 9264–9277.
[213] Ouyang, L., Y. Zhao, G. Jin, T. Lu, J. Li, Y. Qiao, et al. Influence of sulfur content on bone formation and antibacterial ability of sulfonated PEEK. *Biomaterials*, Vol. 83, 2016, pp. 115–126.
[214] Zheng, Y., L. Liu, Y. Ma, L. Xiao, and Y. Liu. Enhanced osteoblasts responses to surface-sulfonated polyetheretherketone *via* a single-step ultraviolet-initiated graft polymerization. *Industrial & Engineering Chemistry Research*, Vol. 57, 2018, pp. 10403–10410.
[215] Wan, T., Z. Jiao, M. Guo, Z. Wang, Y. Wan, K. Lin, et al. Gaseous sulfur trioxide induced controllable sulfonation promoting biomineralization and osseointegration of polyetheretherketone implants. *Bioactive Materials*, Vol. 5, 2020, pp. 1004–1017.
[216] Su, Y., J. He, N. Jiang, H. Zhang, L. Wang, X. Liu, et al. Additively-manufactured poly-ether-ether-ketone (PEEK) lattice scaffolds with uniform microporous architectures for enhanced cellular response and soft tissue adhesion. *Materials and Design*, Vol. 191, 2020, id. 108671.
[217] Xing, P., G. P. Robertson, M. D. Guiver, S. D. Mikhailenko, K. Wang, and S. Kaliaguine. Synthesis and characterization of sulfonated poly(ether ether ketone) for proton exchange membranes. *Journal of Membrane Science*, Vol. 229, 2004, pp. 95–106.
[218] Basile, A., L. Paturzo, A. Iulianelli, I. Gatto, and E. Passalacqua. Sulfonated PEEK-WC membranes for proton-exchange membrane fuel cell: effect of the increasing level of sulfonation on electrochemical performances. *Journal of Membrane Science*, Vol. 281, 2006, pp. 377–385.
[219] Fukuda, N., A. Tsuchiya, R. Toita, K. Tsuru, Y. Mori, et al. Surface plasma treatment and phosphorylation enhance the biological performance of poly(ether ether ketone). *Colloids and Surfaces B: Biointerfaces*, Vol. 173, 2019, pp. 36–42.
[220] Zheng, Y., L. Liu, L. Xiao, Q. Zhang, and Y. Liu. Enhanced osteogenic activity of phosphorylated polyetheretherketone *via* surface-initiated grafting polymerization of vinylphosphonic acid. *Colloids and Surfaces B: Biointerfaces*, Vol. 173, 2019, pp. 591–598.
[221] Liu, L., W. Zhang, L. Yuan, Y. Liu, and Y. Zheng. Ameliorative antibacterial, anti-inflammatory, and osteogenic activity of sulfonate-bearing polyetheretherketone toward orthopedic and dental implants. *Materials Letters*, Vol. 305, 2021, id. 130774.
[222] Petrovic, L., D. Pohle, H. Münstedt, T. Rechtenwald, K. A. Schlegel, and S. Rupprecht. Effect of βTCP filled polyetheretherketone on osteoblast cell proliferationin vitro. *Journal of Biomedical Science*, Vol. 13, 2006, pp. 41–46.
[223] Unarso, S., A. Tsuchiya, R. Toita, K. Tsuru, and K. Ishikawa. Enhanced osseointegration capability of poly(ether ether ketone) *via* combined phosphate and calcium surface-functionalization. *IJMS*, Vol. 21, 2019, id. 198.
[224] Kim, H., Y. H. Lee, N. K. Kim, and I. K. Kang. Immobilization of collagen on the surface of a PEEK implant with monolayer nanopores. *Polymers*, Vol. 14, 2022, id. 1633.
[225] Huo, S., X. Meng, S. Zhang, B. Yue, Y. Zhao, T. Long, et al. Hydrofluoric acid and nitric acid cotreatment for biofunctionalization of polyetheretherketone in M2 macrophage polarization and osteogenesis. *Journal of Biomedical Materials Research*, Vol. 109, 2021, pp. 879–892.
[226] Cao, H., Y. Song, B. Wu, K. Wang, and D. Qu. A force model of high-speed dry milling CF/PEEK considering fiber distribution characteristics. *Journal of Manufacturing Processes*, Vol. 68, 2021, pp. 602–615.
[227] Hassan, E. A. M., D. Ge, S. Zhu, L. Yang, J. Zhou, and M. Yu. Enhancing CF/PEEK composites by CF decoration with polyimide and loosely-packed CNT arrays. *Composites Part A: Applied Science and Manufacturing*, Vol. 127, 2019, id. 105613.
[228] Yan, J.-H., C.-H. Wang, K.-W. Li, Q. Zhang, M. Yang, W.-L. Di-Wu, et al. Enhancement of surface bioactivity on carbon fiber-reinforced polyether ether ketone *via* graphene modification. *IJN*, Vol. 13, 2018, pp. 3425–3440.
[229] Deng, Y., P. Zhou, X. Liu, L. Wang, X. Xiong, Z. Tang, et al. Preparation, characterization, cellular response and in vivo osseointegration of polyetheretherketone/nano-hydroxyapatite/carbon fiber ternary biocomposite. *Colloids and Surfaces B: Biointerfaces*, Vol. 136, 2015, pp. 64–73.
[230] Hahn, B.-D., D.-S. Park, J.-J. Choi, J. Ryu, W.-H. Yoon, J.-H. Choi, et al. Osteoconductive hydroxyapatite coated PEEK for spinal fusion surgery. *Applied Surface Science*, Vol. 283, 2013, pp. 6–11.
[231] Shuai, C., S. Peng, P. Wu, C. Gao, W. Huang, Y. Deng, et al. A nanosandwich construct built with graphene nanosheets and carbon nanotubes enhances mechanical properties of hydroxyapatite–polyetheretherketone scaffolds. *IJN*, Vol. 11, 2016, pp. 3487–3500.
[232] Huang, Z., Y. Wan, X. Zhu, P. Zhang, Z. Yang, F. Yao, et al. Simultaneous engineering of nanofillers and patterned surface macropores of graphene/hydroxyapatite/polyetheretherketone ternary composites for potential bone implants. *Materials Science and Engineering: C*, Vol. 123, 2021, id. 111967.